KDM2A promotes lung tumorigenesis by epigenetically enhancing ERK1/2 signaling

Klaus W. Wagner, … , John V. Heymach, Min Gyu Lee

Research Article   Oncology

Epigenetic dysregulation has emerged as a major contributor to tumorigenesis. Histone methylation is a well-established mechanism of epigenetic regulation that is dynamically modulated by histone methyltransferases and demethylases. The pathogenic role of histone methylation modifiers in non–small cell lung cancer (NSCLC), which is the leading cause of cancer deaths worldwide, remains largely unknown. Here, we found that the histone H3 lysine 36 (H3K36) demethylase KDM2A (also called FBXL11 and JHDM1A) is frequently overexpressed in NSCLC tumors and cell lines. KDM2A and its catalytic activity were required for in vitro proliferation and invasion of KDM2A-overexpressing NSCLC cells. KDM2A overexpression in NSCLC cells with low KDM2A levels increased cell proliferation and invasiveness. KDM2A knockdown abrogated tumor growth and invasive abilities of NSCLC cells in mouse xenograft models. We identified dual-specificity phosphatase 3 (*DUSP3*) as a key KDM2A target gene and found that DUSP3 dephosphorylates ERK1/2 in NSCLC cells. KDM2A activated ERK1/2 through epigenetic repression of *DUSP3* expression via demethylation of dimethylated H3K36 at the *DUSP3* locus. High KDM2A levels correlated with poor prognosis in NSCLC patients. These findings uncover an unexpected role for a histone methylation modifier in activating ERK1/2 in lung tumorigenesis and metastasis, suggesting that KDM2A may be a promising therapeutic target in NSCLC.

Find the latest version:

https://jci.me/68642/pdf

KDM2A promotes lung tumorigenesis by epigenetically enhancing ERK1/2 signaling

Klaus W. Wagner,[1,2] Hunain Alam,[1] Shilpa S. Dhar,[1] Uma Giri,[3] Na Li,[1] Yongkun Wei,[1] Dipak Giri,[4] Tina Cascone,[3] Jae-Hwan Kim,[1] Yuanqing Ye,[5] Asha S. Multani,[6] Chia-Hsin Chan,[1] Baruch Erez,[3] Babita Saigal,[3] Jimyung Chung,[7] Hui-Kuan Lin,[1,8] Xifeng Wu,[5] Mien-Chie Hung,[1,8,9] John V. Heymach,[3,10] and Min Gyu Lee[1,8]

[1]Department of Molecular and Cellular Oncology, [2]Division of Cancer Medicine, and [3]Department of Thoracic/Head and Neck Medical Oncology, The University of Texas MD Anderson Cancer Center, Houston, Texas, USA. [4]Integrated Laboratory Systems, Research Triangle Park, North Carolina, USA. [5]Department of Epidemiology and [6]Department of Genetics, The University of Texas MD Anderson Cancer Center, Houston, Texas, USA. [7]Department of Biochemistry, Yonsei University, Seoul, Republic of Korea. [8]Cancer Biology Program, Graduate School of Biomedical Sciences, The University of Texas Health Science Center, Houston, Texas, USA. [9]Center for Molecular Medicine, China Medical University, Taichung, Taiwan. [10]Department of Cancer Biology, The University of Texas MD Anderson Cancer Center, Houston, Texas, USA.

Epigenetic dysregulation has emerged as a major contributor to tumorigenesis. Histone methylation is a well-established mechanism of epigenetic regulation that is dynamically modulated by histone methyltransferases and demethylases. The pathogenic role of histone methylation modifiers in non–small cell lung cancer (NSCLC), which is the leading cause of cancer deaths worldwide, remains largely unknown. Here, we found that the histone H3 lysine 36 (H3K36) demethylase KDM2A (also called FBXL11 and JHDM1A) is frequently overexpressed in NSCLC tumors and cell lines. KDM2A and its catalytic activity were required for in vitro proliferation and invasion of KDM2A-overexpressing NSCLC cells. KDM2A overexpression in NSCLC cells with low KDM2A levels increased cell proliferation and invasiveness. KDM2A knockdown abrogated tumor growth and invasive abilities of NSCLC cells in mouse xenograft models. We identified dual-specificity phosphatase 3 (*DUSP3*) as a key KDM2A target gene and found that DUSP3 dephosphorylates ERK1/2 in NSCLC cells. KDM2A activated ERK1/2 through epigenetic repression of *DUSP3* expression via demethylation of dimethylated H3K36 at the *DUSP3* locus. High KDM2A levels correlated with poor prognosis in NSCLC patients. These findings uncover an unexpected role for a histone methylation modifier in activating ERK1/2 in lung tumorigenesis and metastasis, suggesting that KDM2A may be a promising therapeutic target in NSCLC.

Introduction

Histone methylation, a key type of histone modification, plays a central role in epigenetic regulation of gene expression at the genome-wide level (1, 2). This modification takes place on arginine and lysine residues and is linked to either activation or repression of gene expression. For example, histone H3 lysine 4 (H3K4), H3K36, and H3K79 methylation marks are commonly associated with gene activation, whereas H3K9, H3K27, and H4K20 methylation marks are generally considered repressive signals. Methylated lysines are present in mono-, di-, or trimethylated states (3, 4). Similar to lysine methylation, arginine methylation occurs at various positions in histones and can exist in monomethylated, symmetrically dimethylated or asymmetrically dimethylated forms (5).

The variety of histone methylation states at several lysine and arginine sites allow for numerous combinatory effects on chromatin dynamics. Methylation has diverse biological and phenotypic consequences, including cellular differentiation, stem cell maintenance, and malignant transformation (3, 4). Lysine methylation is reversibly controlled by histone lysine demethylases (KDMs) and lysine methyltransferases (KMTs). Arginine methylation is known to be catalyzed by arginine protein methyltransferases (PRMTs) (5–7). Recently, it has become evident that a growing number of histone methylation modifiers are dysregulated in tumors and are important for oncogenic phenotypes (8, 9).

Lung cancer is the leading cause of cancer deaths in the United States and worldwide. Non–small cell lung cancer (NSCLC) accounts for about 85% of all lung cancer cases, and its molecular etiology is heterogeneous (10, 11). In particular, cellular kinases (e.g., EGFR, EML4-ALK, PI3K, and c-MET) are frequently mutated and dysregulated in NSCLC, and our understanding of the kinase signaling pathway in NSCLC has been highly advanced (10, 11). Although some kinase signaling pathway members have been targeted for lung cancer therapy, there is still a great need to identify new drug targets that might provide an alternative approach to targeted therapies for NSCLC (10, 11). Therefore, a histone methylation modifier that promotes NSCLC tumorigenesis could be an attractive novel target for drug development. However, the roles that histone methylation modifiers might play in NSCLC tumorigenesis and the kinase signaling pathway remain poorly understood.

To identify histone methylation modifiers that have oncogenic properties in NSCLC, we first investigated which histone methylation modifiers may be highly dysregulated in NSCLC cell lines. Then we determined how a highly dysregulated modifier may contribute to the pathogenesis of NSCLC. In this study, we demonstrate that the histone H3 lysine 36 demethylase KDM2A (also known as FBXL11 and JHDM1A) is overexpressed in a subset of NSCLC and is indispensable for tumorigenicity and invasiveness of KDM2A-overexpressing
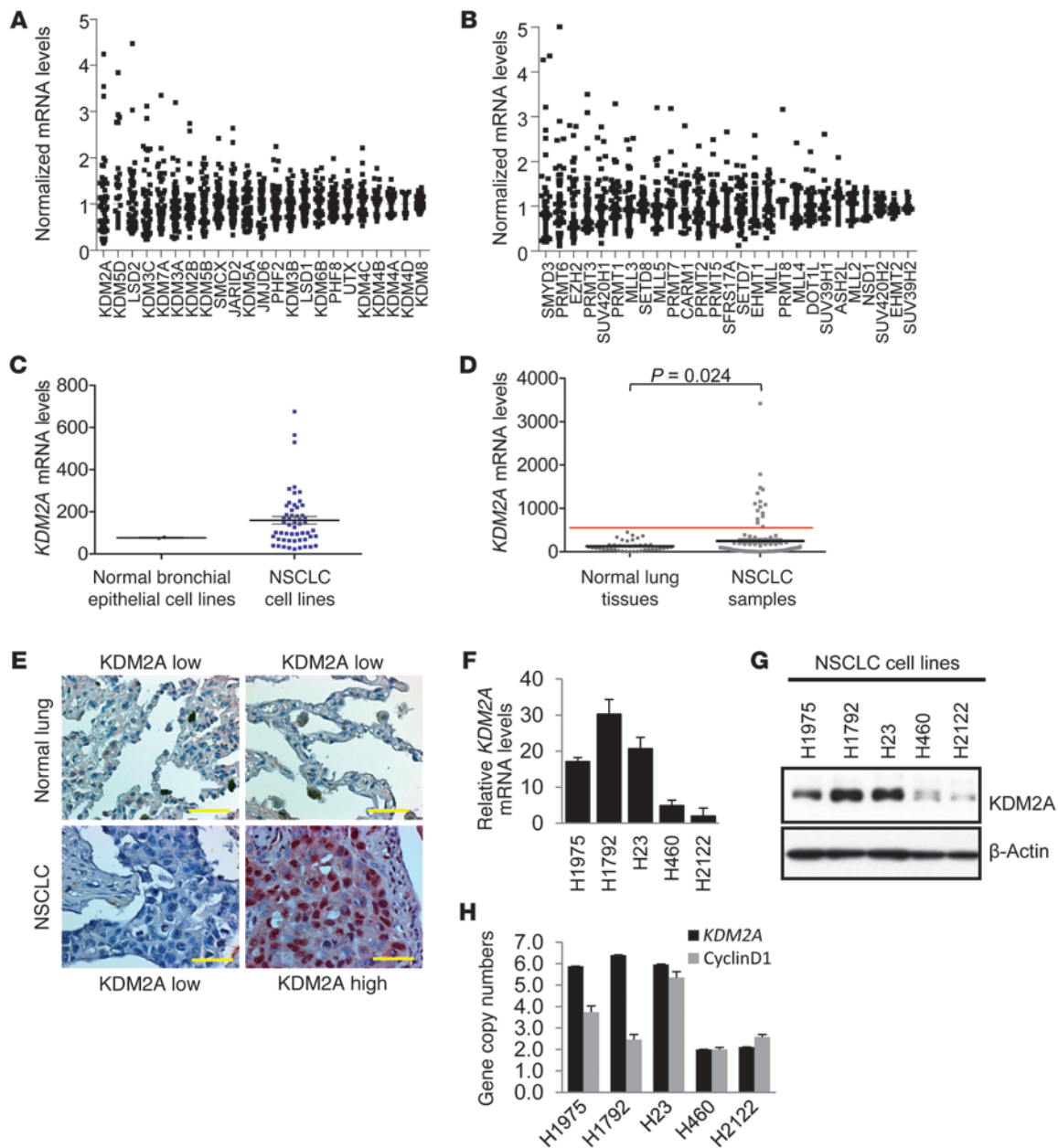
Figure 1

KDM2A levels are frequently increased in NSCLC cell lines and tumors, and the *KDM2A* gene appears to undergo amplification in KDM2A-overexpressing NSCLC cell lines. (**A** and **B**) Expression levels of histone demethylases (**A**) and methyltransferases (**B**) in 54 NSCLC cell lines. The *KDM2A* mRNA levels were determined by Affymetrix U133P microarray analysis (the probe set: 208988_at). (**C**) Comparison of *KDM2A* mRNA levels in 2 normal epithelial cell lines and 54 NSCLC cell lines. *KDM2A* mRNA levels were from Affymetrix U133P microarray data. (**D**) Analysis of *KDM2A* mRNA levels in 103 NSCLC tumors (stages I–III) and 40 adjacent normal lung tissue samples from UT MD Anderson Cancer Center by quantitative RT-PCR. The cut-off value (red line) is 500, which represents the highest normal value among 40 normal lung tissues. The lowest PCR value of *KDM2A* mRNA levels examined was set at 1. (**E**) Representative photographs from IHC analysis of KDM2A protein levels in normal and tumor samples (related to Table 1). Scale bars: 50 μm. (**F** and **G**) Analysis of relative *KDM2A* mRNA and protein levels in 3 KDM2A-overexpressing NSCLC cell lines (H1792, H1975, and H23) and 2 NSCLC cell lines containing low KDM2A levels (H460 and H2122) by quantitative RT-PCR (**F**) and Western blot (**G**), respectively. β-Actin was used as an internal loading control. (**H**) Amplification of *KDM2A* and cyclin D1 genes. Copy numbers of *KDM2A* and cyclin D1 were quantified by DNA PCR.

NSCLC cells. We found that the dual-specificity phosphatase 3 (*DUSP3*) gene, whose protein dephosphorylates ERK1/2, is a primary target of KDM2A-mediated gene repression. Our mechanistic results indicate that KDM2A overexpression activates ERK1/2 by repressing *DUSP3*'s transcription. Thus, these findings provide insights into how the dysregulation of an epigenetic enzyme is coupled to kinase signaling in NSCLC and also reveal the clinical importance of KDM2A in NSCLC.

Table 1

IHC analysis of KDM2A protein levels in 159 NSCLC tumors and 32 normal lung tissues

IHC	KDM2A		
	Low	High	Total
Tissue			
Normal	28 (88%)	4 (12%)	32
NSCLC	95 (60%)	64 (40%)	159
Total	123	68	191

KDM2A high indicates patients with KDM2A protein levels above the mean, whereas KDM2A low denotes the others.

Results

KDM2A levels are frequently upregulated in NSCLC cell lines and tumors. In our search for a histone methylation modifier with oncogenic characteristics for NSCLC, we analyzed expression profiles of 50 histone methylation modifiers (KDMs, KMTs, and PRMTs) using Affymetrix microarray gene expression data for 54 NSCLC cell lines. Mean-normalized SDs were used to rank the histone modifiers because we hypothesized that larger normalized SDs are associated with higher degrees of dysregulation. The expression profile of KDM2A displayed the largest normalized SD within the histone demethylases, whereas SMYD3 was the top candidate within the histone methyltransferases (Figure 1, A and B, and Supplemental Table 1; supplemental material available online with this article; doi:10.1172/JCI68642DS1). For SMYD3, RNAi knockdown experiments indicated that SMYD3 may not be important for the proliferation of SMYD3-overexpressing NSCLC cells (Supplemental Figure 1, A–D). These results led us to choose KDM2A as a primary candidate for subsequent functional analyses.

KDM2A is the first identified jumonji C–containing histone demethylase that removes methyl groups from dimethylated H3K36 (H3K36me2) (12). Because *KDM2A* mRNA levels were higher in a subset of NSCLC cell lines than in normal bronchial epithelial cell lines (Figure 1C), we assessed whether *KDM2A* mRNA levels are upregulated in clinical NSCLC samples. Using quantitative RT-PCR, we measured *KDM2A* mRNA levels of 103 primary NSCLC tumor samples as well as 40 adjacent normal lung tissues from The University of Texas (UT) MD Anderson Cancer Center. *KDM2A* mRNA levels were significantly higher in NSCLC samples than in normal lung tissues. Interestingly, *KDM2A* mRNA levels in about 14% (*n* = 14 out of 103 samples) of NSCLC patients were higher than the highest *KDM2A* mRNA value (500 relative units) in normal tissues (Figure 1D). In addition, immunohistochemistry (IHC) data showed that KDM2A protein levels were significantly increased in an independent set of NSCLC tumor samples (tissue microarray samples) compared with normal tissues (Figure 1E and Table 1). These results indicate that KDM2A is often overexpressed at both mRNA and protein levels in NSCLC patient samples.

The KDM2A gene appears to be amplified in KDM2A-overexpressing NSCLC cell lines and a subset of NSCLC tumors. The *KDM2A* gene is localized at chromosome 11q13.2, whose neighbor region 11q13.3 containing cyclin D1 is amplified in approximately 5% of NSCLC cancer patients (13). To determine whether the *KDM2A* gene undergoes amplification, we examined locus-specific copy numbers of the *KDM2A* and cyclin D1 genes in 3 KDM2A-overexpress-

ing NSCLC cell lines (H1792, H1975 and H23) and 2 NSCLC cell lines (H2122 and H460) with low KDM2A levels (Figure 1, F and G; see also Supplemental Table 2 for the characteristics of these 5 cell lines). Our quantitative DNA PCR analysis revealed that amplification of the *KDM2A* gene occurred only in the 3 KDM2A-overexpressing NSCLC cell lines and did not always coincide with cyclin D1 amplification (Figure 1H). We also performed FISH to confirm *KDM2A* gene amplification in the 3 KDM2A-overexpressing NSCLC cell lines. Normal lymphocytes and an NSCLC cell line (H460) containing low KDM2A levels were used as controls. FISH results showed that *KDM2A* signal numbers were higher in H1792, H1975, and H23 cells than in H460 cells and normal lymphocytes, supporting gene amplification of *KDM2A* in all 3 KDM2A-overexpressing cell lines (Supplemental Figure 2A). Interestingly, Weir et al. reported gene copy number alterations in lung adenocarcinoma using Affymetrix 250K Sty single nucleotide polymorphism arrays (13). Our analysis of their publicly available database indicates that KDM2A may be amplified in a subset of NSCLC tumors (Supplemental Figure 2B).

KDM2A and its enzymatic activity are critical for in vitro proliferation and invasiveness of KDM2A-overexpressing NSCLC cells. To assess whether KDM2A overexpression is important for cell proliferation and invasion, we depleted KDM2A in 3 KDM2A-overexpressing NSCLC cell lines (H1792, H1975 and H23) and 2 NSCLC cell lines (H2122 and H460) with low KDM2A levels using siRNAs (Supplemental Figure 3, A–C). KDM2A knockdown remarkably inhibited the invasiveness of H1792 and H1975 cells (Figure 2, A–D). Moreover, KDM2A depletion substantially reduced the proliferation of all 3 KDM2A-overexpressing NSCLC cell lines (Figure 2, E and F, and Supplemental Figure 4A), whereas it did not affect the proliferation of H460 and H2122 cells (Supplemental Figure 4, B and C). Consistent with these results, KDM2A depletion reduced S phase percentages of H1792 and H1975 cells (Supplemental Figures 5 and 6). Furthermore, KDM2A knockdown reduced colony formation abilities of H1792 and H1975 cells in soft agar (Figure 2, G–I). In contrast, KDM2A knockdown did not have any obvious effect on sub–G1 cell population or caspase 3 cleavage, suggesting that KDM2A may not regulate cellular apoptosis (Supplemental Figures 5–7).

To confirm RNA interference's specificity and to assess whether the enzymatic activity of KDM2A is critical for the phenotypes of KDM2A knockdown cells, we ectopically expressed GFP, wild-type KDM2A, and the catalytic mutant mKDM2A in KDM2A-depleted cells (Supplemental Figure 8, A–D). The rescue experiments demonstrated that only wild-type KDM2A, but not its catalytic mutant mKDM2A (H212A), significantly restored the proliferation of KDM2A-depleted H1792 and H1975 cells (Figure 3, A and B) and almost completely revived their invasiveness (Figure 3, C–F). These results indicate that the function of KDM2A for such cellular characteristics is dependent largely on this enzyme's catalytic activity.

To ensure that KDM2A overexpression is associated with tumor-promoting activities, we stably overexpressed KDM2A in the NSCLC cell line H460 with low endogenous KDM2A levels using a retrovirus-based method. In vitro cellular assays using 2 independent stable clones showed that KDM2A overexpression increased cell proliferation, anchorage-independent growth, and invasiveness of H460 cells (Figure 3, G–L). Together with the above results showing that KDM2A knockdown inhibited cell proliferation and invasiveness of 2 KDM2A-overexpressing cell lines (H1792 and H1975), these results suggest that KDM2A promotes the proliferation and invasiveness of NSCLC cells.
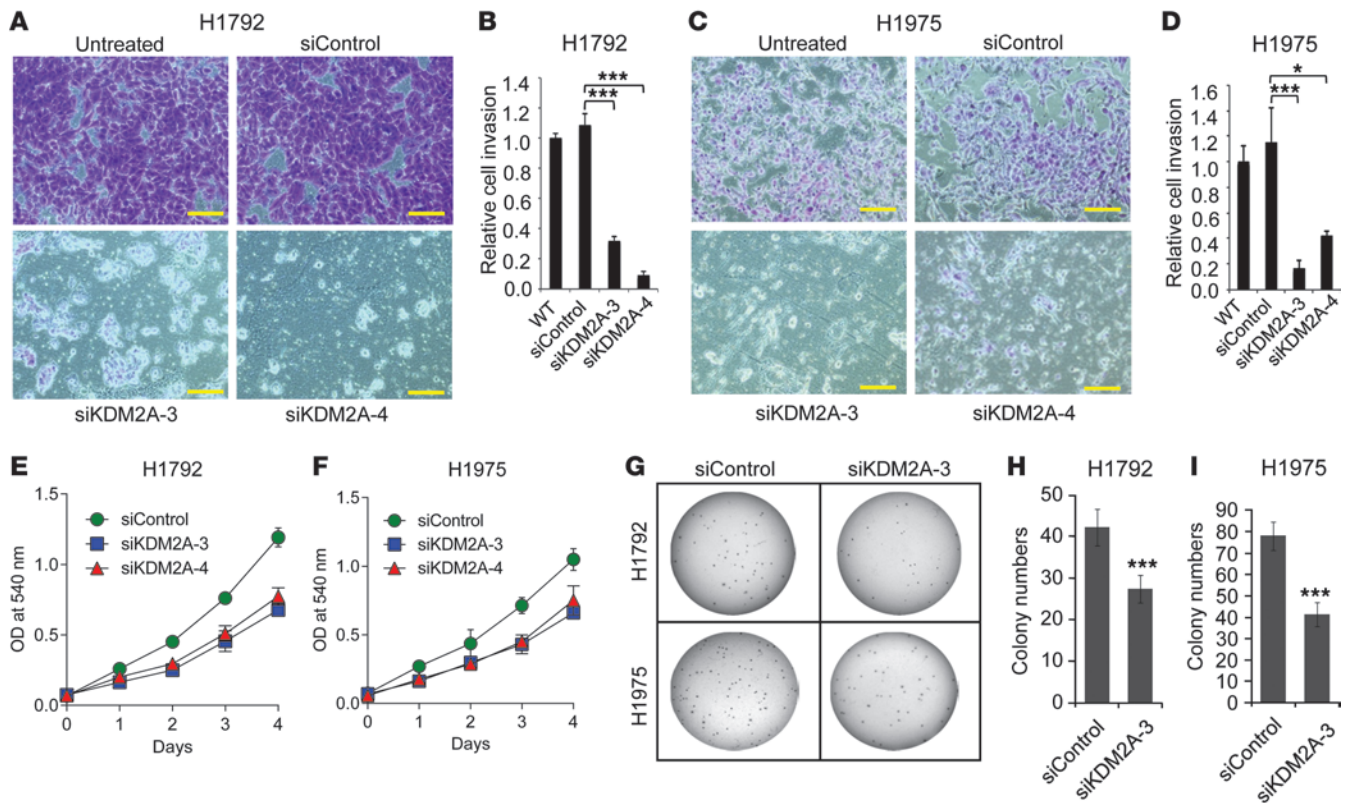
Figure 2
KDM2A is required for the invasiveness, proliferation, and anchorage-independent growth of NSCLC cells. (**A–D**) Effect of KDM2A knockdown on in vitro invasive abilities of 2 KDM2A-overexpressing NSCLC cell lines H1792 (**A** and **B**) and H1975 (**C** and **D**). siControl-treated (siRNA against luciferase) cells were used as controls. Stained cells were quantified in at least 5 different fields (**B** and **D**). (**E** and **F**) Effect of KDM2A knockdown on the proliferation of H1792 (**E**) and H1975 (**F**) cells. Cells were treated with siKDM2A-3 or -4. Cell proliferation was measured by MTT assays. (**G–I**) Effect of KDM2A knockdown on colony formation of H1792 and H1975 cells. Representative pictures are shown (**G**), and colony numbers for H1792 (**H**) and H1975 (**I**) cells were quantified. Scale bars: 400 μm. *$P < 0.05$; ***$P < 0.001$.

The DUSP3 gene is a key target gene of KDM2A. To investigate the mechanisms by which KDM2A may regulate cell proliferation and invasion, we examined the effect of KDM2A knockdown on gene expression profiles. Specifically, we used 2 different siRNAs against KDM2A (siKDM2A-3 or -4) to deplete KDM2A in H1792 and H1975 cells and then compared the mRNA expression levels between KDM2A-depleted cells and control siRNA-treated cells by whole-genome mRNA expression analysis. This analysis identified a list of genes that were consistently up- or downregulated by both siRNAs against KDM2A in both cell lines (Figure 4A and Supplemental Table 3). The total gene number in this list was relatively small, partly because 2 cell lines and 2 different siKDM2As were used to minimize off-target effects and cell line–dependent outcomes of siRNAs. The microarray results of several highly regulated genes and some cancer-related genes, including *DUSP3*, *GPR157*, *TMEM65*, and *TIMM17*, were individually confirmed by quantitative RT-PCR (Figure 4, B and C). Of such genes, DUSP3 expression was notably (up to 9-fold) upregulated by KDM2A knockdown. In addition, DUSP3 has functional implications in tumor suppression (see below). In agreement with KDM2A's effect on mRNA levels of DUSP3, KDM2A depletion also increased DUSP3 protein levels (Figure 4D). In contrast to DUSP3, other DUSP family members were inconsistently or weakly affected by KDM2A knockdown (Supplemental Figure 9).

Recent studies have indicated that KDM2A and its family protein KDM2B are cellular senescence inhibitors in primary mouse embryonic fibroblast (MEF) cells (14). In particular, it has been shown that in MEF cells, KDM2B represses expression of the senescence-associated genes (e.g., *p15^Ink4b*) (15, 16) and modulate p53 and phospho-Rb levels (14). In addition, it has been reported that KDM2B regulates expression of the H3K27 methyltransferase EZH2 and some EZH2-modulated genes (17, 18). Therefore, we assessed whether KDM2A also regulates senescence-associated genes (*p14^ARF*, *p15^Ink4b*, and *p16^Ink4a*), the *EZH2* gene, p53 levels, and phospho-Rb levels. We also included the proapoptotic gene *PUMA* and the cell-cycle inhibitor gene *p21^CIP1* as controls. Quantitative RT-PCR and Western analysis showed that KDM2A knockdown marginally decreased Rb phosphorylation and had no significant effect on *p14^ARF*, *p15^Ink4b*, *p16^Ink4a*, *PUMA*, *p21^CIP1*, and *EZH2* mRNA levels as well as p53 and EZH2 protein levels (Supplemental Figure 10, A–E).

Next, we carried out rescue experiments of KDM2A-regulated genes in KDM2A-depleted cells. Ectopic expression of wild-type KDM2A but not its catalytic mutant mKDM2A significantly repressed the expression of KDM2A-regulated genes, such as *DUSP3* and *TIMM17*, indicating that the demethylase activity of KDM2A is critical in regulating gene expression (Figure 4, E–H).

KDM2A has been implicated in the transcriptional repression of gene expression (19, 20) because it demethylates the gene acti-
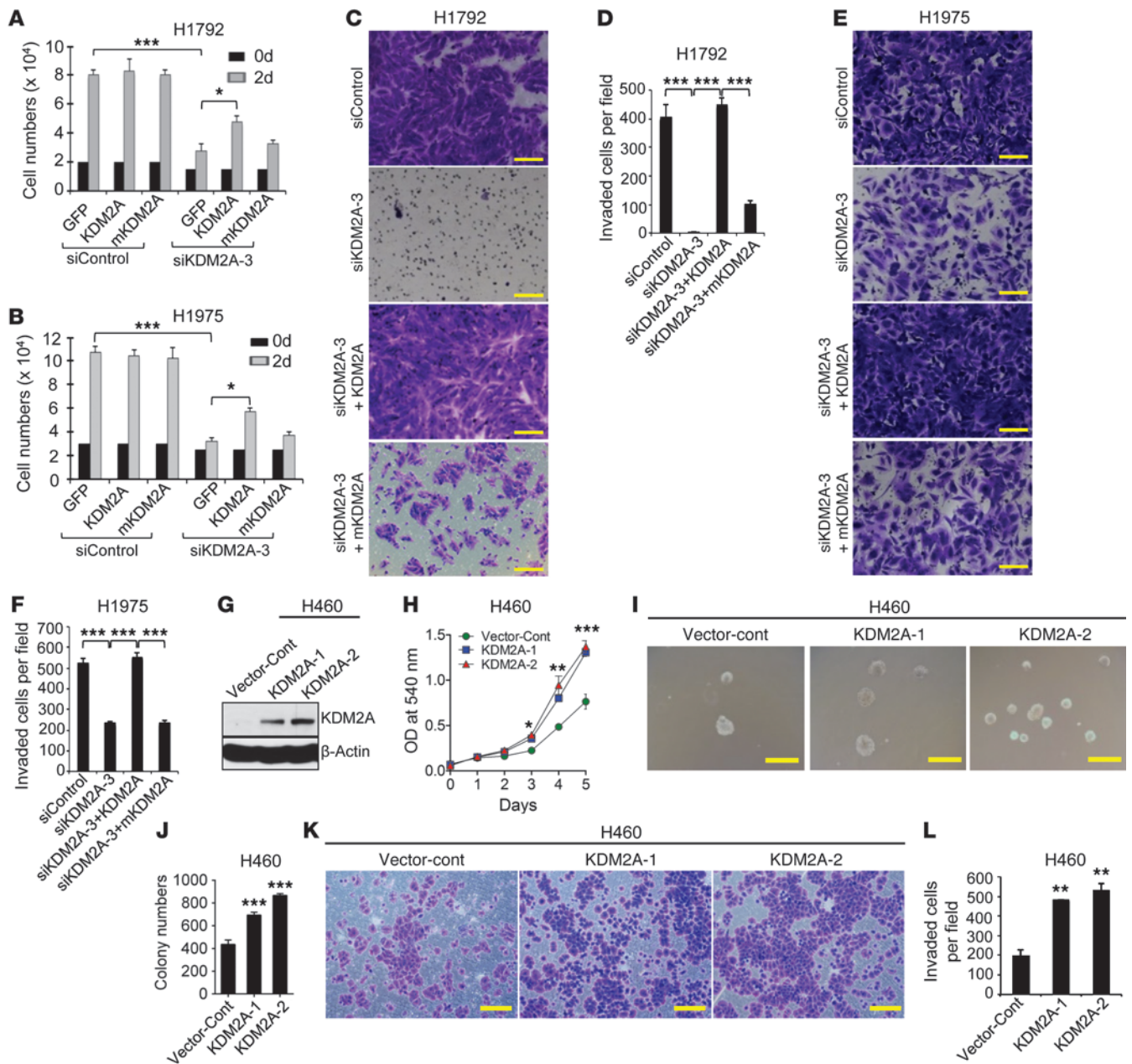
Figure 3
KDM2A's catalytic activity is indispensable for in vitro proliferation and invasiveness of NSCLC cells, and stable KDM2A overexpression promotes cell proliferation, anchorage-independent growth, and cellular invasiveness. (**A** and **B**) Effect of ectopic expression of GFP, wild-type KDM2A, and its catalytic mutant mKDM2A (H212A) on the proliferation of KDM2A knockdown cells. Only wild-type KDM2A rescued defective proliferation of KDM2A-depleted H1792 and H1975 cells. The siControl-treated cells were used as controls. (**C**–**F**) Effect of ectopic expression of GFP, wild-type KDM2A, and its catalytic mutant mKDM2A (H212A) on the defective invasiveness of KDM2A-depleted H1792 (**C** and **D**) and H1975 (**E** and **F**) cells. Cells were treated with siKDM2A-3 to deplete KDM2A. Stained cells were quantified in at least 5 different fields (**D** and **F**). (**G**–**L**) Stable overexpression of KDM2A in H460 NSCLC cells containing low endogenous KDM2A levels. Two KDM2A-overexpressing H460 clones (KDM2A-1 and KDM2A-2) were generated using a retroviral system (**G**). Empty vector–infected cells (vector-cont) were used as control. Cell proliferation was examined by MTT assays (**H**). For colony formation assays, representative phase contrast image of colonies in soft agars are shown (**I**), and colony numbers were quantified (**J**). For in vitro cellular invasion assays, representative images of invaded cells are shown (**K**), and stained cells were quantified in at least 5 different fields (**L**). Scale bars: 200 μm (**C**, **E**, and **K**); 400 μm (**I**). *$P < 0.05$; **$P < 0.01$; ***$P < 0.001$.

vation mark H3K36me2 (21). Therefore, we performed quantitative ChIP experiments to determine whether genes upregulated by KDM2A knockdown are KDM2A target genes. ChIP results showed that KDM2A was recruited to *DUSP3*, *GPR157*, *TMEM65*,

and *TIMM17* genes that were upregulated by KDM2A knockdown in H1975 and H1792 cells (Figure 5, A and B). In contrast, KDM2A did not occupy *GPR107* that was downregulated by KDM2A knockdown (Figure 5, A and B). These results indicate that as a
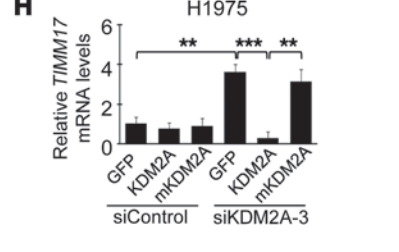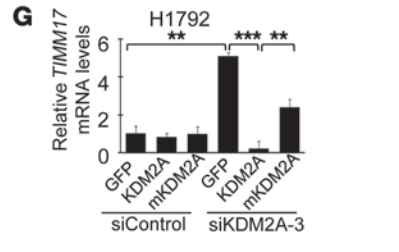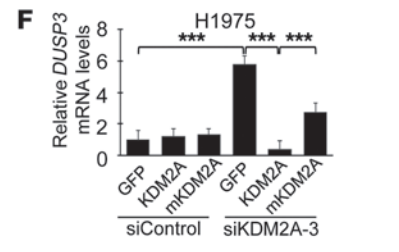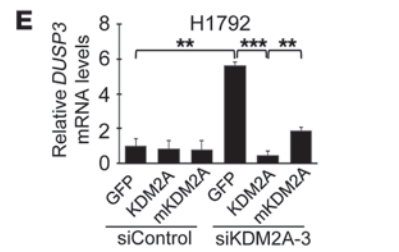
A

H1792 — siControl, siKDM2A-3, siKDM2A-4
H1975 — siControl, siKDM2A-3, siKDM2A-4

>1.5-fold upregulated

siKDM2A-3 — H1792 cell
2079
816 — 109
2092 — 168 — 1126
544 — 575
H1975 cell — 2004 — siKDM2A-4

>2-fold downregulated

siKDM2A-3 — H1792 cell
1426
721 — 109
1319 — 32 — 567
76 — 254
H1975 cell — 550 — siKDM2A-4

Expression (log₂)
low — high
−2.18 — 0.0 — 2.18

B — H1792 — ■ siControl ■ siKDM2A-3
Relative mRNA levels
KDM2A, DUSP3, GPR157, TMEM65, TIMM17, GPR107

C — H1975 — ■ siControl ■ siKDM2A-3
Relative mRNA levels
KDM2A, DUSP3, GPR157, TMEM65, TIMM17, GPR107

D — H1792 — H1975
KDM2A
DUSP3
β-Actin
siControl, siKDM2A-3, siControl, siKDM2A-3

E — H1792
Relative DUSP3 mRNA levels
GFP, KDM2A, mKDM2A — siControl
GFP, KDM2A, mKDM2A — siKDM2A-3

F — H1975
Relative DUSP3 mRNA levels
GFP, KDM2A, mKDM2A — siControl
GFP, KDM2A, mKDM2A — siKDM2A-3

G — H1792
Relative TIMM17 mRNA levels
GFP, KDM2A, mKDM2A — siControl
GFP, KDM2A, mKDM2A — siKDM2A-3

H — H1975
Relative TIMM17 mRNA levels
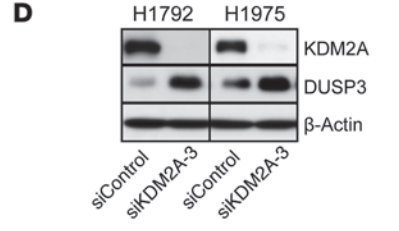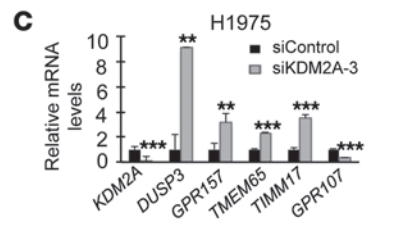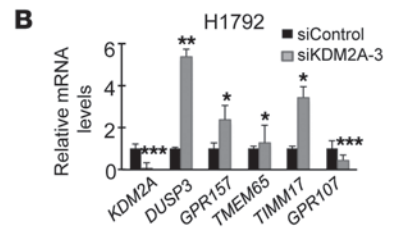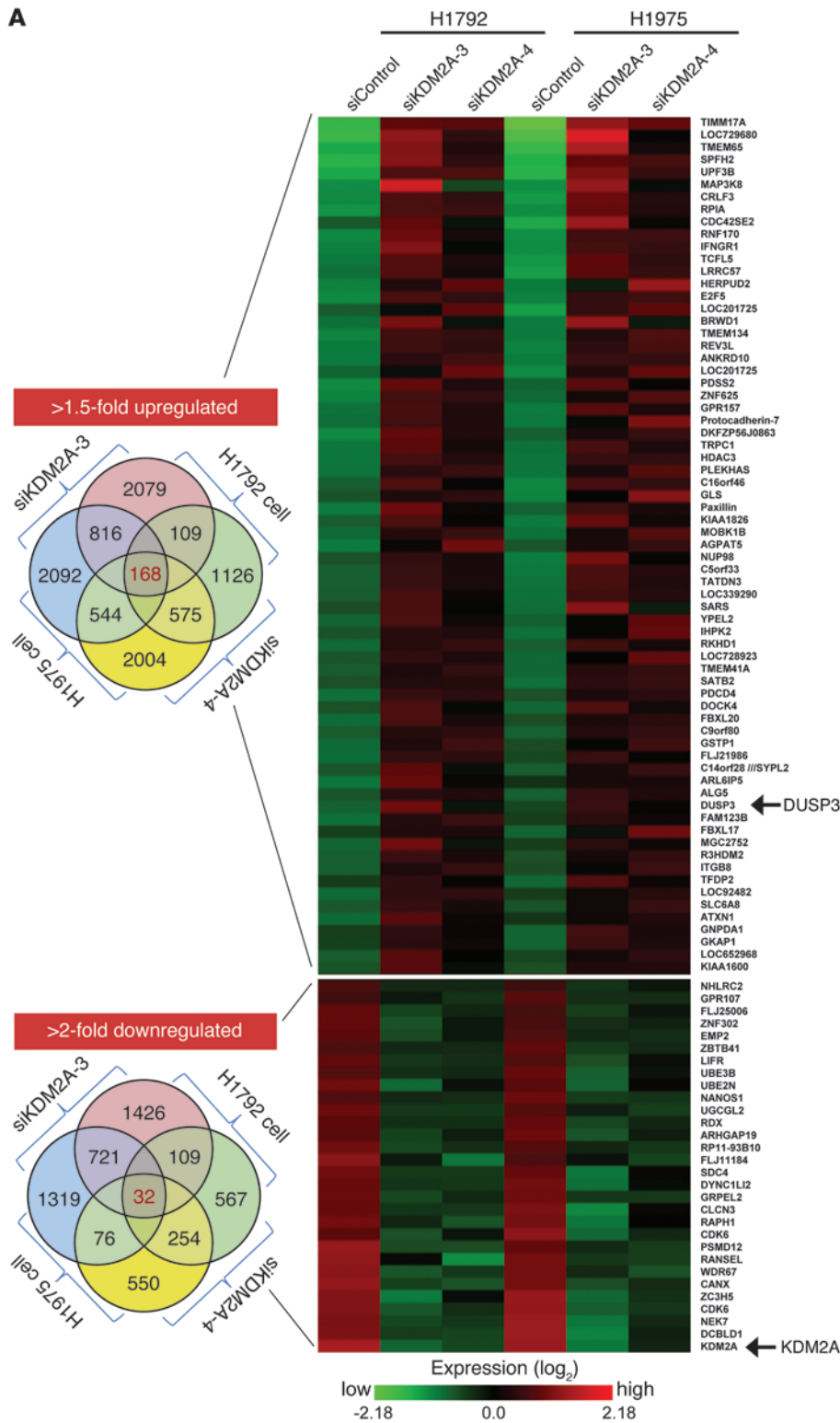GFP, KDM2A, mKDM2A — siControl
GFP, KDM2A, mKDM2A — siKDM2A-3

Figure 4

DUSP3 is highly upregulated by KDM2A knockdown. (**A**) Venn diagrams and a heat map of genes that are consistently 1.5-fold upregulated (top) or 2-fold downregulated (bottom) by KDM2A knockdown. The order of genes in the list does not necessarily reflect the importance of KDM2A-regulated genes because it is based simply on the mean of fold changes in expression that were induced by KDM2A knockdown. H1792 and H1975 cells were treated with siControl, siKDM2A-3, or siKDM2A-4 and harvested 48 hours later. The mRNA levels in KDM2A knockdown cells were measured by Affymetrix U133P and compared with those in siControl-treated cells. (**B** and **C**) Expression levels of *KDM2A*, *DUSP3*, *GPR157*, *TMEM65*, *TIMM17*, and *GPR107* in H1792 (**B**) and H1975 (**C**) cells after KDM2A knockdown. The mRNA levels were analyzed by quantitative RT-PCR. (**D**) The effect of KDM2A knockdown on DUSP3 protein levels. DUSP3 and KDM2A levels were assessed by Western blot analysis using antibodies to DUSP3 in H1792 and H1975 cells. β-Actin was used as an internal loading control. (**E** and **F**) Analysis of *DUSP3* mRNA levels in KDM2A-depleted H1792 (**E**) and H1975 (**F**) cells after ectopic expression of GFP, wild-type KDM2A, and its catalytic mutant mKDM2A (H212A). The *DUSP3* mRNA levels were quantified by RT-PCR. (**G** and **H**) Analysis of *TIMM17* mRNA levels in KDM2A-depleted H1792 (**G**) and H1975 (**H**) cells after ectopic expression of GFP, wild-type KDM2A, and its catalytic mutant mKDM2A (H212A). The *TIMM17* mRNA levels were quantified by RT-PCR. *$P < 0.05$; **$P < 0.01$; ***$P < 0.001$.

transcriptional corepressor, KDM2A directly represses *DUSP3*, *GPR157*, *TMEM65*, and *TIMM17* genes. Together with the above quantitative RT-PCR results showing that *DUSP3* mRNA levels were highly increased by KDM2A knockdown, these data indicate that *DUSP3* is a prominent target gene of KDM2A.

KDM2A-catalyzed demethylation of H3K36me2 occurs at the proximal promoter and the 5′ end of the DUSP3 gene. Because the above results suggest that the potential tumor-suppressor gene *DUSP3* is an important KDM2A target, we focused on understanding the role of DUSP3 in mediating the function of KDM2A. We first performed ChIP assays to determine what regions in the *DUSP3* gene are occupied by KDM2A. ChIP results showed that KDM2A was localized at the proximal promoter (the regions b and c) and the 5′ end (the region d) but not the distal promoter (the region a) in the *DUSP3* gene in H1975 and H1792 cells (Figure 5, C–E). In support of KDM2A's localization at these regions (i.e., b, c, and d) of the *DUSP3* gene, KDM2A knockdown decreased KDM2A levels and increased H3K36me2 levels at the same regions (Figure 5, D–G). Our additional ChIP data demonstrated that total H3 levels at these regions were not changed by KDM2A depletion (Figure 5, H and I) and that KDM2A knockdown did not affect H3K4me3 and H3K27me3 levels at a proximal promoter site (the region c) of the *DUSP3* gene (Figure 5, J and K). These data support that KDM2A-mediated H3K36 demethylation at the *DUSP3* gene may occur near the transcription start site, consistent with a previous report showing that chromatin occupancy peaks of KDM2A are located at the transcription start sites (19). Interestingly, our analyses showed that KDM2A knockdown did not have any significant effect on H3K36me2, H3K4me3, and H3K27me3 levels at the KDM2A's nontarget gene *GPR107* (Figure 5, L and M) and did not affect total cellular levels of H3K36me2 (Supplemental Figure 11), suggesting that KDM2A-caztalyzed H3K36 demethylation occurs in a gene-specific manner. Taken together, these results indicate that KDM2A specifically demethylates H3K36me2 at the proximal promoter and the 5′ end of the

DUSP3 gene and also suggests that KDM2A-catalyzed demethylation of H3K36me2 at the *DUSP3* gene is coupled to KDM2A-mediated transcriptional repression of *DUSP3*.

Epigenetic repression of DUSP3 by KDM2A antagonizes DUSP3-mediated dephosphorylation of ERK1/2. DUSP3 has been shown to suppress the activities of ERK1/2 and JNK1/2 in HeLa cells and the activity of EGFR in the lung cancer cell line H1299 by dephosphorylating these kinases (22–25). ERK1/2 and JNK1/2 are a family of MAPKs that play a critical role in mediating cellular signaling events, including cell proliferation and invasion (26–29). Moreover, ERK1/2 has been described as an important oncogenic factor for NSCLC (30). We assessed whether increased levels of DUSP3 by KDM2A knockdown have an effect on phosphorylation levels of ERK1/2, JNK1/2, and EGFR. The MAPK p38 and the key serine-threonine protein kinase AKT1 were also examined as controls. Western blot analysis showed that increases in DUSP3 levels by KDM2A knockdown dramatically decreased phospho-ERK1/2 levels and moderately downregulated phospho-JNK1/2 levels without affecting phosphorylation levels of EGFR, p38, and AKT (Figure 6A and Supplemental Figure 12, A and B). Ectopic overexpression of DUSP3 in H1792 cells drastically reduced phospho-ERK1/2 and phospho-JNK1/2 levels (Figure 6B). Interestingly, stable overexpression of KDM2A in H460 cells containing low endogenous KDM2A levels upregulated phospho-ERK1/2 but not phospho-JNK1/2 levels (Figure 6C). In an effort to examine whether ERK1/2 phosphorylation affects the proliferation and invasion of KDM2A-overexpressing NSCLC cells, we treated H1792 cells with the MEK1/2 inhibitor U0126 (10 μM), which has been widely used to consequently impede ERK1/2 phosphorylation. These in vitro assays showed that continuous inhibition of ERK1/2 phosphorylation by U0126 decreased both cellular properties (Supplemental Figure 13, A–C). These results indicate that KDM2A-mediated repression of DUSP3 expression primarily increases ERK1/2's phosphorylation (an important regulator for cell proliferation and invasion) in NSCLC cells while upregulating JNK1/2's phosphorylation in a cell-type–dependent manner.

To determine whether increased levels of DUSP3 by KDM2A knockdown also lead to decreased phospho-ERK1/2 levels during cellular signaling, we serum-starved siControl- or siKDM2A-treated H1792 cells, reintroduced serum into the cell-culture medium, and compared phospho-ERK1/2 levels between control cells and KDM2A knockdown cells during serum activation. KDM2A knockdown increased DUSP3 levels and delayed phosphorylation of ERK1/2 without affecting phosphorylation levels of p38 and EGFRs (Figure 6D and Supplemental Figure 14A). These results indicate that KDM2A negatively regulates DUSP3 levels and consequently inhibits DUSP3-catalyzed dephosphorylation of ERK1/2 during serum-induced signaling in NSCLC cells.

KDM2A regulates cell growth and invasiveness in a DUSP3-dependent manner. To determine whether KDM2A regulates ERK1/2 in a DUSP3-dependent manner, we depleted DUSP3 in KDM2A knockdown H1792 cells and serum-starved these double-knockdown cells in addition to control cells and KDM2A-only knockdown cells. After reintroducing serum into the culture medium, we compared phospho-ERK1/2 levels among these 3 groups of H1792 cells during serum activation. Analysis of phospho-ERK1/2 levels showed that DUSP3 knockdown restored phospho-ERK1/2 levels in KDM2A-depleted cells (Figure 6E). Next, we examined the effect of DUPS3 knockdown on the proliferation and invasiveness of KDM2A-depleted cells. DUSP3 knock-
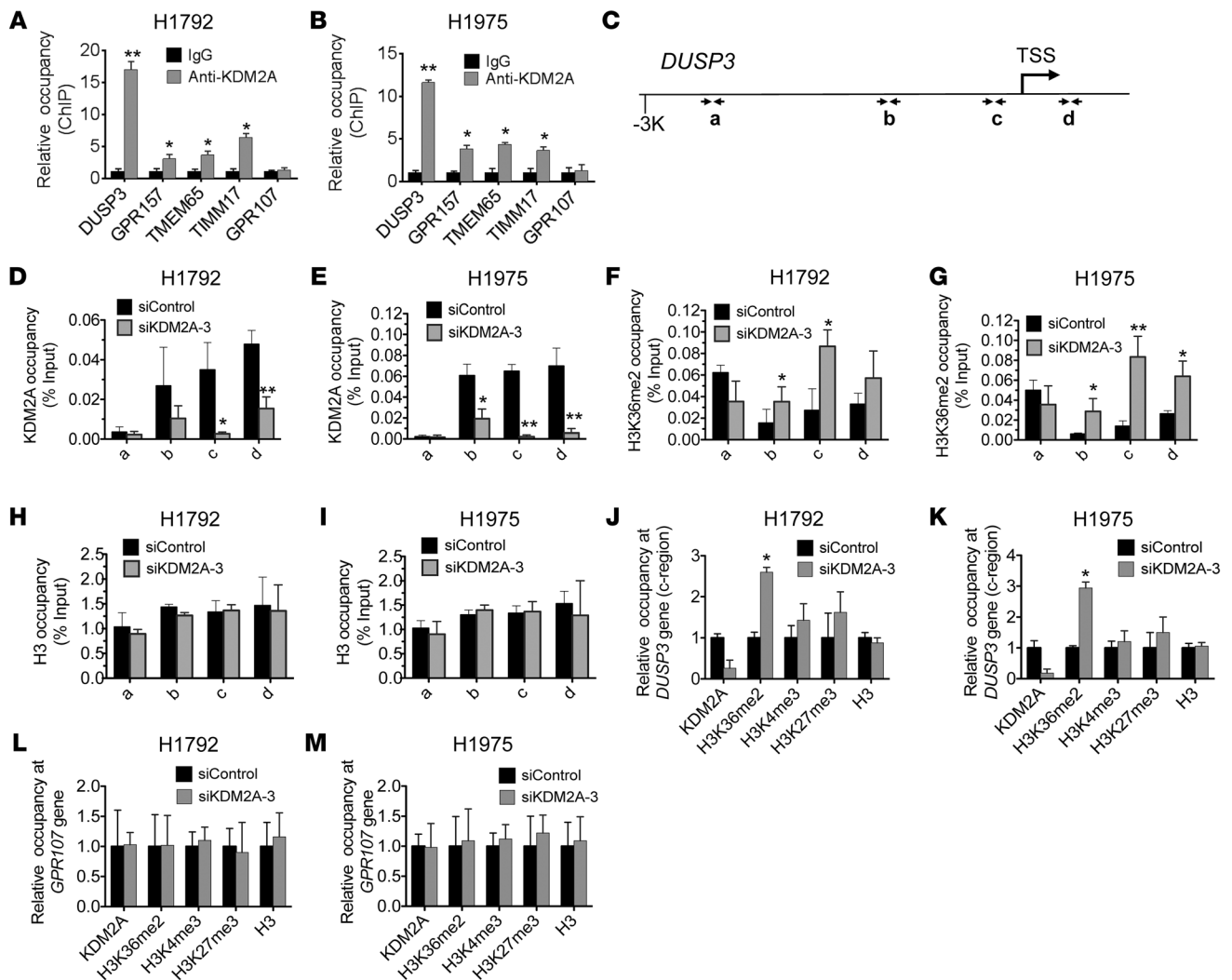
Figure 5

KDM2A demethylates H3K36me2 at the proximal promoter and the 5′ end of the *DUPS3* gene. (**A** and **B**) Analysis of occupied levels of KDM2A at the *DUSP3*, *GPR157*, *TMEM65*, *TIMM17*, and *GPR107* genes in H1792 (**A**) and H1975 (**B**) cells. Chromatin levels of KDM2A were measured by quantitative ChIP. (**C**) Diagrammatic representation of the distal promoter region (a), and the proximal promoter regions (b and c), and the 5′ end (d) of the *DUSP3* gene. Arrows indicate the PCR-amplified regions. TSS, transcription start site. (**D**–**I**) Analysis of occupied levels of KDM2A (**D** and **E**), H3K36me2 (**F** and **G**), and H3 (**H** and **I**) at the *DUSP3* gene in H1792 (**D**, **F**, and **H**) and H1975 (**E**, **G**, and **I**) cells. Chromatin levels of KDM2A, H3K36me2, and H3 were measured by quantitative ChIP. (**J**–**M**) Analysis of occupied levels of KDM2A, H3K36me2, H3K4me3, H3K27me3, and H3 at the promoter region in the *DUSP3* gene (**J** and **K**) and at the *GPR107* gene (**L** and **M**) in H1792 (**J** and **L**) and H1975 (**K** and **M**) cells. Chromatin levels of KDM2A, H3K36me2, H3K4me3, H3K27me3, and H3 were measured by quantitative ChIP. For direct comparison, KDM2A levels of the region c in **D** and **E** are replotted in **J** and **K**. Anti-H3 was used as a ChIP control. *$P < 0.05$; **$P < 0.01$.

down significantly restored defective proliferation of KDM2A-depleted cells and remarkably increased their invasiveness (Figure 6, F and G, and Supplemental Figure 14B). These results suggest that the proliferation and invasiveness of KDM2A-over-expressing NSCLC cells are dependent largely on the epigenetic repression of DUSP3 levels by KDM2A.

It has been shown that DUSP3 is localized in either the nucleus or the cytosol in a cell type–specific manner (31). Our cell fraction-ation analysis demonstrated that DUSP3 was localized exclusively in the cytosol in H1792 and H1975 cells, suggesting that dephos-phorylation of ERK1/2 by DUSP3 occurs in cytosol of NSCLC cells (Figure 6H and Supplemental Figure 14C).

KDM2A is critical for tumor growth and invasion in mouse xenograft models. To address the role of KDM2A in NSCLC tumorigenesis in vivo, we treated KDM2A-overexpressing H1792 cells with con-trol siRNA, siKDM2A-3, or siKDM2A-4 and injected cells into tail veins of mice (in intravenous mouse xenograft models, cancer cells primarily colonize the lung and form tumors there). This intra-venous mouse xenograft experiment demonstrated that all mice ($n = 4/4$) that were injected with control siRNA–treated H1792 cells had multiple bilateral lung tumors within 4 months, whereas no mice that were injected with KDM2A-depleted cells showed signs of lung tumor growth by NSCLC cells ($n = 0/6$) (Figure 7A and Table 2). Lung tumors were confirmed by H&E staining (Figure 7B).
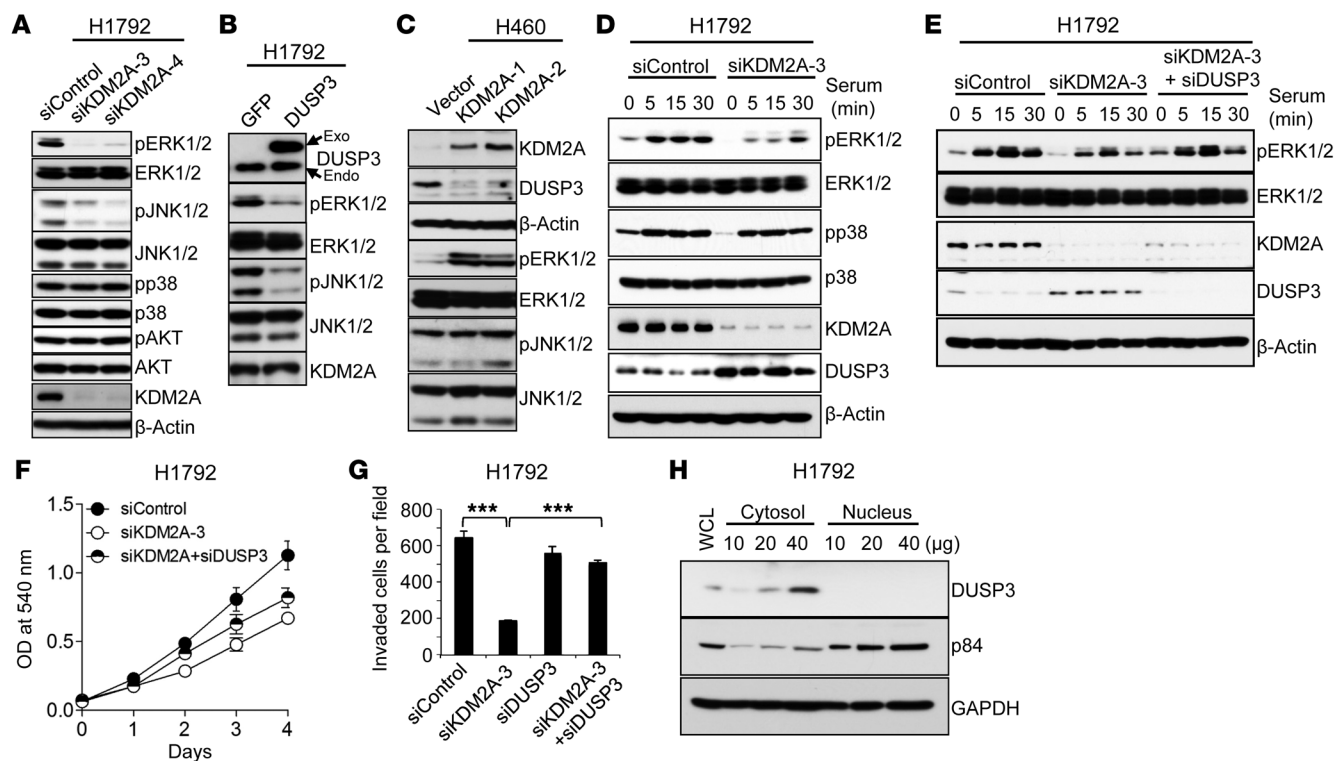
Figure 6
The transcriptional repression of *DUSP3* by KDM2A reduces DUSP3-catalyzed dephosphorylation of ERK1/2 and contributes to the proliferation and invasiveness of NSCLC cells. (**A**) Effect of KDM2A knockdown on phosphorylation levels of ERK1/2 and JNK1/2. H1792 cells treated with siControl or siKDM2As were examined by Western blot analysis. (**B**) Effect of DUSP3 overexpression on phosphorylation levels of ERK1/2 and JNK1/2. H1792 cells transfected with GFP-expression (a control) or DUSP3-expression plasmid were examined by Western blot analysis. Exo, exogenous; Endo, endogenous. (**C**) Effect of KDM2A overexpression on phospho-ERK1/2 and phospho-JNK1/2 in H460 cells with low endogenous KDM2A levels. (**D**) Effect of KDM2A knockdown on phospho-ERK1/2 levels during serum activation. KDM2A-depleted H1792 cells and control cells were stimulated with 10% serum for 5, 15, or 30 minutes after 18 hours of serum starvation. Protein extracts were then examined by Western blot analysis. (**E**) Effect of double knockdown of KDM2A and DUSP3 on phosphorylation levels of ERK1/2 during serum activation. Control, KDM2A-depleted, and DUSP3/KDM2A-depleted H1792 cells were stimulated as in **D**. (**F**) Rescue of the proliferation defect of KDM2A-depleted H1792 cells by DUSP3 knockdown. (**G**) Rescue of the invasive defect of KDM2A-depleted H1792 cells by DUSP3 knockdown. (**H**) Cytosolic localization of DUSP3 in H1792 cells. Cytoplasmic and nuclear fractions were examined by Western blot analysis. GAPDH and p84 were used as a loading control and a nuclear marker, respectively. WCL, whole cell lysates.

We further assessed the tumorigenic role of KDM2A by implanting KDM2A-depleted H1792 cells into the mouse lung parenchyma. This orthotopic lung experiment showed that KDM2A knockdown remarkably inhibited tumor formation in lungs and completely abrogated the invasion of cancer cells to hilar and mediastinal lymph nodes and contralateral lungs (Figure 7, C and D, Supplemental Figure 15, and Table 3). These results indicate that KDM2A may be required for in vivo tumor growth and invasion of NSCLC cells.

To confirm the above mouse xenograft experiments on the basis of siRNA-treated cells in which siRNA-mediated knockdown is transient, we sought to determine the effect of stable KDM2A knockdown on tumor growth. We first treated H1792 cells with 2 different shRNAs against KDM2A using a lentiviral system and generated 2 stably KDM2A-depleted cell lines. Similar to siRNA-based results, shRNA-mediated stable knockdown of KDM2A increased DUSP3 levels and decreased phospho-ERK1/2 levels and cell proliferation (Figure 8, A and B). We next assessed tumor growth abilities of these 2 stably KDM2A-depleted cell lines using a mouse xenograft model on the basis of subcutaneous injec-

tion. Stable knockdown of KDM2A almost completely eradicated tumor growth (Figure 8, C and D, and Table 4). In support of this, IHC analysis showed that a tiny tumor from stably KDM2A-depleted cells had high DUSP3 levels and low phospho-ERK1/2 levels as compared with tumors from shControl-treated cells (Figure 8E). In comparison with these subcutaneous mouse xenograft results on the basis of stable KDM2A knockdown, we also examined the effects of transient KDM2A knockdown on tumor growth in the same mouse xenograft model. As compared with stable knockdown, transient KDM2A depletion by siRNAs moderately decreased tumor volumes (Supplemental Figure 16, A–D). These results confirmed not only the inhibitory effect of KDM2A knockdown on tumor growth but also demonstrated that stable KDM2A knockdown more profoundly inhibited tumor growth than siKDM2A-mediated knockdown did.

High KDM2A protein levels are associated with poor prognosis. To investigate whether KDM2A overexpression is relevant to the clinical outcome of NSCLC patients, we performed Kaplan-Meier survival analysis of the tumor sample set from UT MD
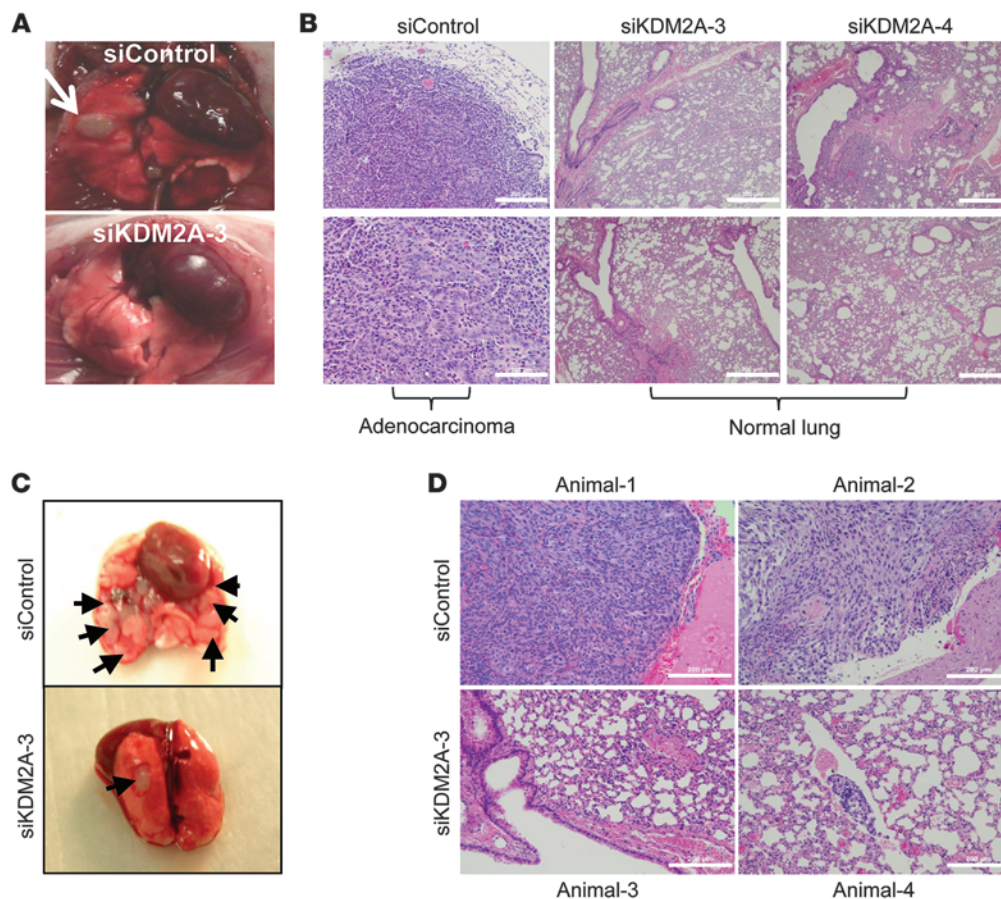
Figure 7

KDM2A is essential for tumor growth and metastasis of NSCLC cells in vivo. (**A** and **B**) Effect of KDM2A knockdown on lung tumor colonization in an intravenous mouse xenograft model. H1792 cells treated with siControl RNA or 2 siRNAs against KDM2A were injected into mouse tail veins, and lung tumor formation was monitored. Representative gross images of lung show a lung-metastasized tumor (white arrow) in a control siRNA group mouse as compared with a tumor-free lung from a siKDM2A-3 group mouse (**A**). H&E-stained microscopic images display lung-metastasized tumor (adenocarcinoma) in a control siRNA group mouse in contrast with tumor-free normal lung histology in siKDM2A group mice (**B**). (**C** and **D**) Effect of KDM2A knockdown on formation of metastatic lesions in an orthotopic lung mouse xenograft model. H1792 cells treated with siControl or siKDM2A-3 were implanted into the parenchyma of left lung, and the contralateral lungs and lymph nodes were monitored for metastasis. Representative gross images of lung show massive multiple tumors (arrows) in a control siRNA group mouse as compared with a tiny tumor in a siKDM2A group mouse (**C**). H&E-stained microscopic images display massive tumors in control siRNA group mice in contrast with none or a miniscule tumor in siKDM2A group mice (**D**). Scale bars: 200 μm.

Anderson Cancer Center (see Figure 1D). This analysis based on mRNA levels demonstrated that high *KDM2A* mRNA levels (≥500 relative units) were associated with poor survival of these patients ($P = 0.0015$) (Figure 8F). In addition, we determined whether IHC-based KDM2A protein levels are associated with poor survival. Survival analysis was performed using 76 NSCLC tumor samples with clinical history out of 191 IHC-analyzed samples that were used for Table 1. Our analysis based on IHC-based KDM2A levels also demonstrated that patients (*n* = 38) with high levels of KDM2A protein displayed poor overall survival (Figure 8G). Interestingly, there was no significant correlation between KDM2A overexpression and patient age, sex, smoking status, histologic subtypes, or clinical stage in either tumor sets, except node status in IHC-based KDM2A levels (Supplemental Tables 4 and 5). These results indicate that KDM2A may be a prognostic biomarker independent of clinical parameters and histologic NSCLC subtypes.

High KDM2A levels significantly correlate with low DUSP3 and high phospho-ERK levels. Because KDM2A upregulates phospho-ERK1/2 by repressing DUSP3 expression in NSCLC cell lines, we sought to determine whether there is any correlation among KDM2A, DUSP3, and phospho-ERK1/2 levels in NSCLC tumor samples. Based on IHC analysis (Figure 9A), KDM2A levels inversely correlated with DUSP3 levels (Table 5) and were positively associated with phospho-ERK1/2 levels (Table 6). In addition, we analyzed the relationship between KDM2A and DUSP3 on the basis of mRNA levels using both a publicly available microarray dataset for 443 lung adenocarcinoma (stages I–III) from the NCI Director's Challenge Consortium (32) and the tumor samples from UT MD Anderson Cancer Center (see Figure 1D). These analyses showed that *KDM2A* and *DUSP3* mRNA levels had a significant inverse correlation in both datasets, although the tumor dataset from UT MD Anderson Cancer

Table 2

Comparison of lung tumor development between siControl group and siKDM2A groups in an intravenous xenograft mouse model

Treatment (i.v.)	Mice (*n*)	Mice (*n*) with lung tumors
siControl	4	4 (100%)
siKDM2A-3	3	0 (0%)
siKDM2A-4	3	0 (0%)

H1792 cells treated with siControl, siKDM2A-3, or siKDM2A-4 were injected into mouse tail veins, and lung tumor colonization was examined.

Center displayed a much lower correlation (perhaps, due to the low number of samples) (Supplemental Figure 17, A and B). In contrast to higher *KDM2A* mRNA levels in NSCLC tumors, *DUSP3* mRNA levels were significantly lower in NSCLC tumor samples than in normal lung tissues (Supplemental Figure 17C).

We examined whether low DUSP3 or high phospho-ERK1/2 levels are related to the clinical outcomes of NSCLC patients. Kaplan-Meier survival analysis on the basis of IHC showed that low DUSP3 or high phospho-ERK1/2 protein levels were associated with poor survival (Figure 9, B and C). Similarly, low *DUSP3* mRNA levels showed a trend (albeit not significant) for poor prognosis (Supplemental Figure 18A). In addition, our combinatorial survival analysis demonstrated that high KDM2A levels with low DUSP3 levels, high KDM2A levels with high phospho-ERK1/2 levels, and high KDM2A levels with low DUSP3 and high phospho-ERK1/2 levels correlated with poor patient survival (Figure 9, D and E, and Supplemental Figure 18, B and C). Together, these results suggest that high KDM2A levels are linked to low DUSP3 and high phospho-ERK levels in patient tumor samples.

Discussion

In the present study, our results indicate that KDM2A is critical for the proliferation and invasion of KDM2A-overexpressing NSCLC cells in vitro and in vivo. Our work also indicates that the addiction of tumor growth and invasiveness of NSCLC cells to KDM2A depends mainly on KDM2A's enzymatic activity. Importantly, we identified *DUSP3* as a primary target of KDM2A. Our data support the notion that KDM2A increases phospho-ERK1/2 levels by epigenetically downregulating expression of *DUSP3*. These findings suggest that activation of ERK1/2 by KDM2A-mediated repression of *DUSP3* is linked to tumorigenesis and metastasis of NSCLC cells (Figure 9F).

Several activating mutations or genomic aberrations of kinase signaling pathway members (e.g., KRAS and EGFR) are related to tumorigenesis and commonly activate MAPK signaling (10). However, the role of a histone methylation modifier in regulating the oncogenic MAPK signaling pathway has been not well described. Intriguingly, results reported here indicate that KDM2A-catalyzed demethylation augments ERK1/2's oncogenic activities via transcriptional repression of *DUSP3*, supporting the notion that the epigenetic activity of KDM2A is coupled to ERK1/2 signaling. Consistent with this, we showed that DUSP3 knockdown in KDM2A-depleted cells rescued phospho-ERK1/2 levels during serum activation while restoring the growth and invasiveness of KDM2A-depleted cells. In addition, our IHC

analysis of NSCLC tumor samples demonstrated that high KDM2A levels correlate with high phospho-ERK1/2 or low DUSP3 levels. Furthermore, our IHC-based survival analysis indicated that low DUSP3 or high phospho-ERK1/2 is linked to poor prognosis. In contrast to DUSP3-mediated regulation of ERK1/2, our analysis of other known DUSP3 substrates demonstrated that phospho-EGFR and phospho-p38 levels were not regulated by DUSP3, while DUSP3-mediated dephosphorylation of phospho-JNK1/2 appeared to occur in an NSCLC cell type–dependent manner. Thus, our findings reveal a previously unidentified mechanism in which a histone methylation modifier primarily activates ERK1/2 by antagonizing DUSP3-mediated dephosphorylation of ERK1/2 via epigenetic repression of *DUSP3*.

KDM2A has been shown to regulate somatic cell reprogramming and cellular senescence (14, 33). Distinct from these cellular functions of KDM2A, our in vitro cellular experiments in this study demonstrated that KDM2A knockdown inhibited the proliferation, anchorage-independent growth, and invasiveness of KDM2A-overexpressing NSCLC cells. In addition, our in vivo mouse xenograft models showed that tumor growth and invasive abilities of KDM2A-overexpressing NSCLC cells were abrogated by KDM2A depletion. In line with these results, we also found that stable KDM2A overexpression in an NSCLC cell line (H460) containing low KDM2A levels promoted cell proliferation, colony formation abilities in soft agar, and cellular invasiveness. These findings suggest that KDM2A is required for and promotes NSCLC's growth and metastasis.

KDM2A's requirement for the proliferation and invasiveness of KDM2A-overexpressing NSCLC cells is in accordance with the oncogene addiction model in which the growth and survival of cancer cells can be suppressed by inactivation of single oncogenes (34). Overexpression of certain oncogenes, such as EGFR and HER2, is linked to poor clinical outcomes. Our current study demonstrated that, similar to such oncogenes, high expression levels of KDM2A correlated with poor prognosis in 2 independent NSCLC patient populations: an NSCLC tumor set from UT MD Anderson Cancer Center (*n* = 98) and a commercially available NSCLC tumor set (*n* = 76). Overexpression of oncogenes is often accompanied by gene amplification. For example, several receptor tyrosine kinases, including EGFR and HER2, undergo gene amplification in NSCLC (10). Our results indicate that the *KDM2A* gene is likely amplified in KDM2A-overexpressing NSCLC cells, supporting KDM2A's oncogenic characteristics. In addition to such NSCLC cell lines, *KDM2A* gene amplification may occur in patients' NSCLC samples with high KDM2A levels because our analysis of a publicly available database suggests

Table 3

Effect of siRNA-mediated KDM2A knockdown on tumor formation and metastasis in an orthotopic xenograft mouse model of lung cancer

Treatment	Mice (*n*)	Mice (*n*) with lung tumors	Mice (*n*) with metastasis	
			Contralateral lung	Mediastinal lymph node
siControl	6	6	3	3
siKDM2A-3	6	3	0	0

H1792 cells treated with siControl or siKDM2A-3 were injected into the left lung. At the 13th week after injection, the contralateral lungs and lymph nodes were examined for metastatic tumors.
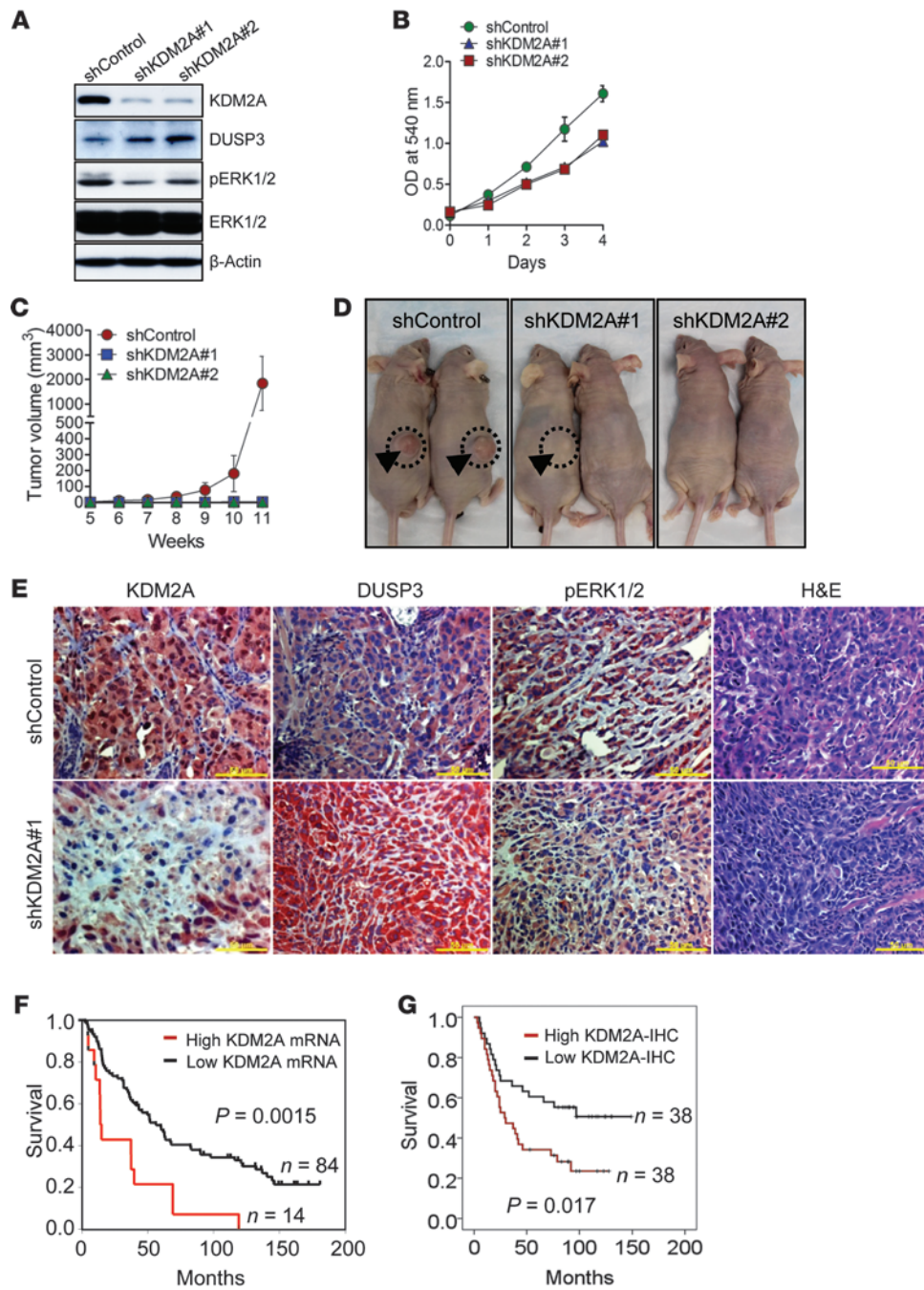
Figure 8
Stable knockdown of KDM2A drastically inhibits tumor growth of NSCLC cells in vivo, and high KDM2A correlates with poor prognosis of lung cancer patients. (**A–E**) The effect of stable knockdown of KDM2A on tumor growth ability of NSCLC cells in a subcutaneous mouse xenograft model. Stably KDM2A-depleted H1792 cells were generated using shK–DM2A#1- and shKDM2A#2–containing viruses. KDM2A, DUSP3, and phospho-ERK1/2 levels were determined by Western blot analysis (**A**). Cell proliferation was measured by MTT assays (**B**). Stable KDM2A knockdown (shKDM2A#1 and shKDM2A#2) cells and control cells (shLuciferase) were subcutaneously injected into mice ($n = 5$ for each group). Tumor development was monitored and plotted for 11 weeks (**C**). Representative pictures of tumors developed in nude mice are shown, and tumors are indicated by black arrows in dotted circles (**D**). Representative images of IHC staining (anti-KDM2A, anti-DUSP3, and anti–phospho-ERK1/2) and H&E staining of tumor tissues are shown (**E**). Scale bars: 50 μm. (**F**) Kaplan-Meier survival rate analysis of the tumor set from UT MD Anderson Cancer Center. Tumor samples with patient history ($n = 98$ out of 103 samples; see Figure 1D) were classified as high KDM2A or low KDM2A by a cut-off value of 500. (**G**) Survival rate analysis of an NSCLC patient set on the basis of KDM2A protein levels measured by IHC ($n = 76$). From tumor samples in Table 1, KDM2A high ($n = 38$) and KDM2A low ($n = 38$) with patient history were used for this analysis.

KDM2A gene amplification in a subset of NSCLC tumors (Supplemental Figure 2B). Thus, it is tempting to speculate that the amplification of the *KDM2A* gene may be a mechanism underlying KDM2A overexpression in NSCLC. Together, our results suggest oncogenic properties for KDM2A in NSCLC tumorigenesis.

Overexpression of KDM2A or its family protein KDM2B has been shown to immortalize MEF cells (14). Of interest, KDM2B has been linked to p53/Rb and cellular senescence pathway (14). The molecular mechanisms underlying the role of KDM2B in increasing p53 and phospho-Rb levels remain unclear, but KDM2B was shown to repress cellular senescence–related genes, including *p15^{Ink4b}* and *p16^{Ink4a}* (15, 16). KDM2B was also reported to regulate *EZH2* expression via miRNA101 repression and

to coregulate some EZH2 target genes (17, 18). However, results presented here showed that KDM2A knockdown had no robust effect on Rb phosphorylation and expression levels of *p53*, *EZH2*, and key cellular senescence–related genes (i.e., *p14^{ARF}*, *p15^{Ink4b}*, and *p16^{Ink4a}*) in NSCLC cells. In addition, KDM2A may not affect cellular apoptosis, because our assays showed that *PUMA* expression, sub-G1 cell population, and caspase 3 cleavage were not modulated by KDM2A knockdown. Thus, it is possible that in NSCLC cells, KDM2A may increase cell proliferation by activating ERK1/2 rather than by inhibiting cellular senescence and apoptosis.

In the current study, our data showed that DUSP3 knockdown significantly restored in vitro proliferative and invasive abilities of KDM2A-depleted cells, suggesting that DUSP3 is a critical

Table 4
Effect of stable KDM2A knockdown on tumor formation in a subcutaneous xenograft mouse model

Treatment (s.c.)	Mice (*n*)	Mice (*n*) with tumors
shControl	5	4
shKDM2A#1	5	1
shKDM2A#2	5	1

Stably KDM2A-depleted (shKDM2A#1 and shKDM2A#2) cells and control cells (shControl) were subcutaneously implanted into mice. At the 11th week after injection, numbers of tumor-bearing mice were counted.

target of KDM2A. We also demonstrated that low DUSP3 levels had a significant correlation with high KDM2A levels and often occurred in NSCLC tumors. In line with our results, it has been shown that DUSP3 is downregulated in NSCLC and that DUSP3 overexpression leads to decreased cell proliferation and reduced tumor growth in a xenograft mouse model (24). Together with this

previous report, our findings indicate a tumor-suppressive role for DUSP3 in NSCLC and suggest that the epigenetic repression of DUSP3's tumor-suppressive function by KDM2A contributes to NSCLC tumor growth and invasiveness.

The majority of NSCLC patients do not have well-defined drug targets, such as EGFR and ALK. It is also challenging that most of NSCLC patients who receive targeted therapies (e.g., the EGFR inhibitor erlotinib) eventually acquire drug resistance (10, 11). Therefore, the identification of new drug targets may provide better therapeutic options for NSCLC patients. It is known that genetic abnormalities of KRAS and EGFR in NSCLC frequently converge on the same downstream effectors, such as ERK1/2 (10, 11). In this regard, our results indicate that KDM2A overexpression activates key downstream effectors (i.e., ERK1/2) in kinase-signaling pathways via epigenetic repression of *DUSP3* and therefore provide a rationale for KDM2A-targeted therapy for patients with KDM2A-overexpressing NSCLC. Moreover, our findings may be highly relevant to future studies of the role of KDM2A in the pathogenesis of other cancer types because KDM2A appears to be
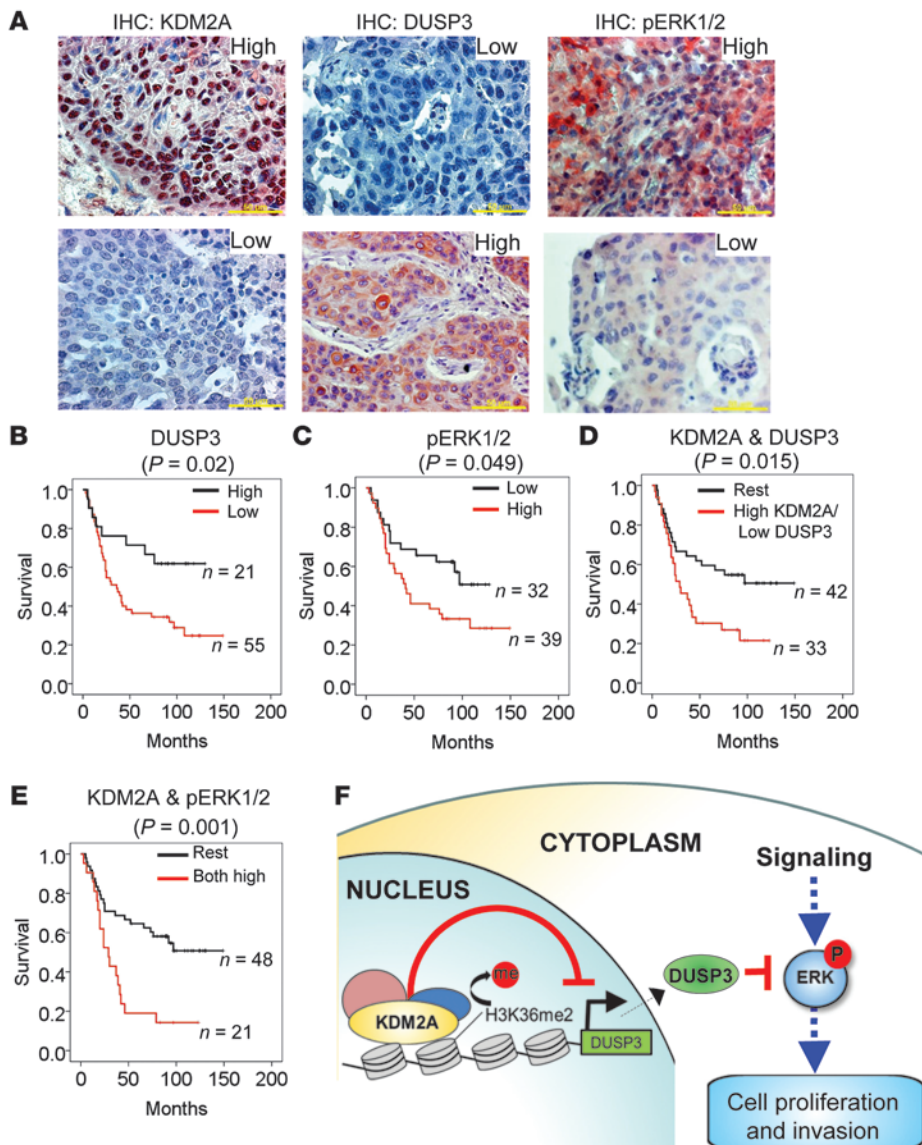

Figure 9
In NSCLC tumors, high KDM2A levels are associated with low DUSP3 and high phospho-ERK levels, which are related to poor prognosis. (**A**) Representative images of IHC staining of NSCLC tumors with anti-KDM2A, anti-DUSP3, and anti–phospho-ERK1/2. Scale bars: 50 μm. (**B** and **C**) Kaplan-Meier survival rate analysis for DUSP3 (**B**) and phospho-ERK1/2 (**C**) levels measured by IHC. (**D** and **E**) Kaplan-Meier survival rate analysis using different combination of KDM2A, DUSP3, and phospho-ERK1/2 levels on the basis of IHC (i.e., high KDM2A with low DUSP3 vs. rest [**D**], high KDM2A with high phospho-ERK1/2 vs. rest [**E**]). Tumor samples with patient history (see Supplemental Table 5) were used for survival analysis of **B**–**E**. (**F**) A hypothetical representation of the regulatory pathway underlying KDM2A-promoted cell proliferation and invasion. The phosphatase DUSP3 specifically dephosphorylates ERK1/2 in NSCLC cells. KDM2A represses the *DUSP3* gene by removing the epigenetic activation mark H3K36me2. KDM2A-mediated repression of *DUSP3* results in increased phospho-ERK1/2 levels, which are critical for cell proliferation and invasiveness. Thus, activation of ERK1/2 by KDM2A-mediated repression of *DUSP3* contributes to the proliferation and metastasis of NSCLC cells. me, methyl group; p, phosphorylated.

Table 5

Correlation analysis between high KDM2A and low DUSP3 levels
in 93 human NSCLC tumor samples by IHC

IHC	DUSP3		
KDM2A	Low	High	Total
Low	29	19	48
High	40	5	45
Total	**69**	**24**	**93**

P = 0.002, based on the χ^2 test.

overexpressed in breast and pancreatic cancer (data not shown). Finally, KDM2A may be used as a biomarker for poor prognosis because high KDM2A levels are associated with poor survival in 2 distinct NSCLC patient cohorts.

Methods

Samples, reagents, and antibodies. For IHC, formalin-fixed and paraffin-embedded tissue microarray samples were obtained from Biomax (LC951 and LC1291) and Imgenex (IMH-305) and processed as described in the manufacturers' instructions. All NSCLC cell lines were purchased from ATCC. Cell culture reagents were purchased from Invitrogen (Gibco); all other chemicals were from Sigma-Aldrich. The KDM2A-specific antibodies were purchased from Novus (NB100-74602 for Western blot analysis) and Abgent (AP1043c for IHC). Antibodies to phospho-ERK1/2, ERK1/2, phospho-JNK1/2, JNK1/2, phospho-p38, p38, phospho-AKT, AKT, phospho-EGFRs, EGFR, EZH2, Caspase3, DUSP3, phospho-Rb, and Rb were from Cell Signaling. Antibodies to H3K36me2 were from Active Motif, and antibodies to H3K36me3 and H3 were from Abcam. Antibodies to DUSP3 (for IHC) and β-actin were from Abgent and Sigma-Aldrich, respectively. HRP-conjugated anti-mouse-IgG, HRP-conjugated anti-rabbit-IgG, and anti-p53 were from Santa Cruz Biotechnology Inc.

Microarrays and data analysis. Total cellular RNA from 54 NSCLC cell lines was prepared. Oligonucleotide microarrays consisting of 54,613 gene probes (U133P GeneChip; Affymetrix) were used for hybridization. Probe set 208988_at was used to examine mRNA expression of KDM2A. For analysis of genes regulated by KDM2A, 2 cell lines (H1792 and H1975) were treated with 2 different siKDM2As (siKDM2A-3 and -4). After 48 hours of siRNA treatment, cells were harvested. In an effort to minimize any indirect modulation of gene expression by a prolonged KDM2A knockdown, we chose 48 hours as a relatively short incubation time point. Expression levels of KDM2A knockdown cells were measured by Affymetrix U133P and compared with those of siControl-treated cells. The NCI Director's Challenge Consortium data for the Molecular Classification of Lung Adenocarcinoma represents publicly available Affymetrix U133A microarray data set of tumor samples from 443 lung NSCLC adenocarcinoma patients (stage I–III) (32).

Quantitative RT-PCR. For quantitative RT-PCR, 103 NSCLC samples and 40 normal lung tissue samples were collected. The presence or absence of NSCLC was verified by histological examination. NSCLC tumors included adenocarcinoma, squamous cell carcinoma, and large cell carcinoma (stages I–III). Messenger RNA was isolated using the RNeasy Kit (QIAGEN). Single-stranded cDNA was synthesized using the iScript cDNA Synthesis Kit (Bio-Rad). Quantitative PCR was performed in triplicates using the CFX96 real-time system (Bio-Rad) as previously described (35). Specific primers for *KDM2A*, *18S rRNA* (control), and other genes were designed (see Supplemental Table 6). The relative mRNA levels indicate the fold change over the control.

IHC. The avidin-biotin immunoperoxidase method was used for deparaffinized zinc formalin-fixed, paraffin-embedded sections, which were purchased from Biomax and Imgenex. Slides placed in citrate buffer were heated in a microwave oven for 20 minutes prior to the application of the primary antibodies (such as anti-KDM2A, anti-DUSP3 and anti-phospho-ERK1/2) for 1 hour at room temperature. Evaluation of staining intensity was carried out by the Chromavision Automated Cellular Imaging System (ACIS-III) from Dako.

Analysis of gene copy number. Quantitative DNA-PCR was performed using ABI real-time PCR equipment (StepOnePlus). Fluorescence signals emitted from FAM dye were detected using ABI TaqMan copy number assays as the dye was released from the probe during amplification. For each test sample, triplicate wells were set up for *KDM2A*, cyclin D1, and a reference control gene RNAse *P* on a different chromosome.

FISH. FISH was performed to identify the copy number changes of KDM2A in H1792, H1975, H23, and H460 NSCLC cell lines. The BAC clone (RP11-268F16) containing KDM2A /FBXL11 and the chromosome 11 α satellite centromere clone were labeled by nick translation with Spectrum Red and Spectrum Green, respectively (Abbott Laboratories). Hybridization and detection were performed according to the manufacturer's protocols. The slides were counterstained with DAPI, and the images were captured using Nikon 80i microscope equipped with a cooled-charge coupled devices (CCD) camera. A total of 100 interphase nuclei were analyzed to determine the amplification status. Lymphocytes that were cultured from a healthy male were used as a control.

RNAi and transfection protocol. siRNAs against KDM2A were purchased from Dharmacon and Sigma-Aldrich. The selected siRNA sequences were as follows: siKDM2A-3, 5′ AA-CAAGGAGAGUGUGGGUGUUU-dTdT 3′; siKDM2A-4, 5′ AA-UUACGAAGCCUCACACUAU-dTdT 3′; siDUSP3, 5′ AA-CCCUGUAAAGUUAGUAGAGCUUg-dTdT 3′. As controls, siRNA against luciferase *GL3* RNA (5′ AACTTACGCTGAGTACTTCGA-dTdT 3′) or a FITC-conjugated siRNA from Dharmacon were used. Cells (5 × 10⁴) in a 6-well plate were transfected with siRNAs at a final concentration of 100 nM using Lipofectamine RNAiMAX (Invitrogen). Following 72 to 96 hours incubation, cells were harvested for mRNA and protein analysis or used for cell proliferation and invasion assays.

Cell proliferation assay. Cells were seeded at a density of 1500 to 2000 cells per well in 96-well plates and treated with control siRNA or siKDM2A at a final concentration of 20–100 nM; relative cell numbers were determined at 1–4 days after treatment according to MTS protocol (Promega).

Cell invasion assay. To assess in vitro invasive abilities of tumor cells, the Boyden chamber assay, one of the most commonly used in vitro invasion assays, was performed using inserts with membrane (8-μm pore size). In brief, 1.0×10^5 cells (in 500 μl serum-free medium) were seeded on the Matrigel coated on the membrane of the inserts that were placed in 500 μl serum-containing medium in the well of a 24-well plate. Eighteen hours later, cells that invaded the Matrigel and migrated to the other side of the membrane were stained and counted.

Table 6

Correlation analysis between high KDM2A and high
phospho-ERK1/2 levels in human NSCLC tumor samples by IHC

IHC	phospho-ERK1/2		
KDM2A	Low	High	Total
Low	26	23	49
High	11	29	40
Total	**37**	**52**	**89**

P = 0.018, based on the χ^2 test.

Generation of stably KDM2A-overexpressed H460 cells and KDM2A-depleted H1792 cells. To investigate the effect of KDM2A overexpression on cell growth, invasion, and anchorage-independent growth, KDM2A was overexpressed in H460 NSCLC cells with low endogenous KDM2A levels using the pMarXG KDM2A retrovirus construct (a gift of Howard Green, Harvard Medical School, Boston, USA). Single-cell clones were isolated, expanded in medium containing 2 μg/ml puromycin (Sigma-Aldrich), and screened for the overexpression of KDM2A using Western blot analysis. Two KDM2A-overexpressing H460 clones (KDM2A-1 and KDM2A-2) were selected. Empty vector–infected cells were used as control. To generate stable KDM2A knockdown cells, H1792 cells were infected with shKDM2A#1– and shKDM2A#2–containing viruses (Sigma-Aldrich). Cells were selected in 2 μg puromycin containing medium. Empty vector–infected cells were used as control.

Soft agar assay. In addition to H1792, H1975 cells and their KDM2A-depleted cells, H460 cells and their derivatives were tested for anchorage-independent growth using a colony formation assay based on soft agar. In brief, 1 ml of 1% agar in complete RPMI was plated as the basal layer in 6-well plates. Cells (1×10^4) in complete medium containing 0.4% agar were seeded on the basal layer. Plates were incubated at 37°C in a CO_2 incubator for 14 days. Opaque, dense colonies were microscopically examined and counted at the 14th day. The assays were repeated 3 times in 3 replicates.

Expression constructs and rescue experiments by ectopic expression. The cDNA constructs encoding KDM2A, its catalytic mutant mKDM2A (H212A), or GFP were cloned into the mammalian expression vector pFLAG-CMV2 using standard cloning methodology. Eukaryotic expression plasmids (2 μg) were transfected into either siControl- or siKDM2A-treated cells (2–5×10^5 cells) in 60-mm dishes using 10 μl of Lipofectamine 2000 (Invitrogen). These cells were harvested after 72 hours for further analysis. Total RNAs were isolated and analyzed by quantitative RT-PCR.

Quantitative ChIP assay. ChIP assays were performed using Millipore ChIP assay protocol with minor modifications. DNA was purified from chromatin fragments immunoprecipitated by antibodies and amplified by quantitative PCR using specific primer sets for individual genes (see Supplemental Table 6). PCR values were normalized to input and calculated as percentage of input. Relative occupancy indicates the fold change in percentage of input over the control (e.g., anti-KDM2A/IgG).

Stimulation of MAPK signaling by serum. To study the activation of MAPK signaling, cells were treated with control siRNA, siKDM2A, or a combination of siKDM2A and siDUSP3, serum-starved for 18 hours, and then treated with 10% serum for 0, 5, 15, or 30 minutes. Proteins were extracted for Western blot analysis.

Mouse xenograft studies. Female or male nu/nu mice were purchased from Charles River Laboratory or UT MD Anderson Cancer Center. Mice were injected with H1792 cells (1×10^6) that were treated with control siRNA or siKDM2As for 72 hours. For each group, 3–6 mice were used as follows: siControl ($n = 4$), siKDM2A-3 ($n = 3$), and siKDM2A-4 ($n = 3$) for tail vein injection; siControl ($n = 6$) and siKDM2A-3 ($n = 6$) for orthotopic lung injection. For the intravenous mouse xenograft model, mice were sacrificed at the 4th, 8th, and 13th weeks after injection. For the orthotopic mouse xenograft model, mice were sacrificed at the 13th week after injection, and the lungs and lymph nodes were inspected for metastasis, which were confirmed by H&E staining. To further determine the effect of KMD2A knockdown on tumorigenicity of H1792 cells, 2×10^6 cells were subcutaneously injected into the dorsal flank of 6- to 8-week-old nude mice as previously described (36). Control or KDM2A-depleted H1792 cells were suspended in RPMI without serum before injection. At least 5 mice were injected for each group and observed for 11 to 12 weeks for tumor formation. The ellipsoid volume formula ($1/2 \times l \times w \times h$) was used to calculate the tumor volume.

Statistics. The χ^2 test was used for correlation analysis. Statistical significance of survival analysis was tested by the log-rank (Mantel-Cox) method. The data were analyzed with the Statistical Package SPSS 19.0 for Windows (SPSS Inc.). Two groups of data were statistically analyzed by 2-tailed t test using Graphpad Prism 5 Software. A P value of less than 0.05 was considered statistically significant. Data are presented as the mean ± SEM.

Study approval. For mRNA measurement, NSCLC and adjacent tissues were collected after formal informed consents under Institutional Review Board approval at the UT MD Anderson Cancer Center. The care and use of all mice were approved by MD Anderson's Animal Care Committee.

Address correspondence to: Min Gyu Lee, Department of Molecular and Cellular Oncology, Unit 108, The University of Texas MD Anderson Cancer Center, 1515 Holcombe Blvd., Houston, Texas 77030, USA. Phone: 713.792.3678; Fax: 713.794.3270; E-mail: mglee@mdanderson.org.

1. Barski A, et al. High-resolution profiling of histone methylations in the human genome. *Cell.* 2007;129(4):823–837.
2. Mikkelsen TS, et al. Genome-wide maps of chromatin state in pluripotent and lineage-committed cells. *Nature.* 2007;448(7153):553–560.
3. Sims RJ, Nishioka K, Reinberg D. Histone lysine methylation: a signature for chromatin function. *Trends Genet.* 2003;19(11):629–639.
4. Martin C, Zhang Y. The diverse functions of histone lysine methylation. *Nat Rev Mol Cell Biol.* 2005;6(11):838–849.
5. Bedford MT, Clarke SG. Protein arginine methylation in mammals: who, what, and why. *Mol Cell.* 2009;33(1):1–13.
6. Shi Y, Whetstine JR. Dynamic regulation of histone lysine methylation by demethylases. *Mol Cell.* 2007;25(1):1–14.
7. Klose RJ, Zhang Y. Regulation of histone methylation by demethylimination and demethylation. *Nat Rev Mol Cell Biol.* 2007;8(4):307–318.
8. Dawson MA, Kouzarides T. Cancer epigenetics: from mechanism to therapy. *Cell.* 2012;150(1):12–27.
9. Shi Y. Histone lysine demethylases: emerging roles in development, physiology and disease. *Nat Rev Genet.* 2007;8(11):829–833.
10. Herbst RS, Heymach JV, Lippman SM. Lung cancer. *N Engl J Med.* 2008;359(13):1367–1380.
11. Sharma SV, Bell DW, Settleman J, Haber DA. Epidermal growth factor receptor mutations in lung cancer. *Nat Rev Cancer.* 2007;7(3):169–181.
12. Tsukada Y, et al. Histone demethylation by a family of JmjC domain-containing proteins. *Nature.* 2006;439(7078):811–816.
13. Weir BA, et al. Characterizing the cancer genome in lung adenocarcinoma. *Nature.* 2007; 450(7171):893–898.
14. Pfau R, Tzatsos A, Kampranis SC, Serebrennikova OB, Bear SE, Tsichlis PN. Members of a family of JmjC domain-containing oncoproteins immortalize embryonic fibroblasts via a JmjC domain-dependent process. *Proc Natl Acad Sci U S A.* 2008;

105(6):1907–1912.

15. He J, Kallin EM, Tsukada Y, Zhang Y. The H3K36 demethylase Jhdm1b/Kdm2b regulates cell proliferation and senescence through p15(Ink4b). *Nat Struct Mol Biol*. 2008;15(11):1169–1175.

16. Tzatsos A, Pfau R, Kampranis SC, Tsichlis PN. Ndy1/KDM2B immortalizes mouse embryonic fibroblasts by repressing the Ink4a/Arf locus. *Proc Natl Acad Sci U S A*. 2009;106(8):2641–2646.

17. Tzatsos A, et al. KDM2B promotes pancreatic cancer via Polycomb-dependent and -independent transcriptional programs. *J Clin Invest*. 2013; 123(2):727–739.

18. Kottakis F, Polytarchou C, Foltopoulou P, Sanidas I, Kampranis SC, Tsichlis PN. FGF-2 regulates cell proliferation, migration, and angiogenesis through an NDY1/KDM2B-miR-101-EZH2 pathway. *Mol Cell*. 2011;43(2):285–298.

19. Blackledge NP, Zhou JC, Tolstorukov MY, Farcas AM, Park PJ, Klose RJ. CpG islands recruit a histone H3 lysine 36 demethylase. *Mol Cell*. 2010; 38(2):179–190.

20. Frescas D, et al. KDM2A represses transcription of centromeric satellite repeats and maintains the heterochromatic state. *Cell Cycle*. 2008;7(22):3539–3547.

21. Kuo AJ, et al. NSD2 links dimethylation of histone H3 at lysine 36 to oncogenic programming. *Mol Cell*. 2011;44(4):609–620.

22. Todd JL, Tanner KG, Denu JM. Extracellular regulated kinases (ERK) 1 and ERK2 are authentic substrates for the dual-specificity protein-tyrosine phosphatase VHR. A novel role in downregulating the ERK pathway. *J Biol Chem*. 1999; 274(19):13271–13280.

23. Todd JL, Rigas JD, Rafty LA, Denu JM. Dual-specificity protein tyrosine phosphatase VHR downregulates c-Jun N-terminal kinase (JNK). *Oncogene*. 2002;21(16):2573–2583.

24. Wang JY, et al. Vaccinia H1-related phosphatase is a phosphatase of ErbB receptors and is downregulated in non-small cell lung cancer. *J Biol Chem*. 2011;286(12):10177–10184.

25. Rahmouni S, et al. Loss of the VHR dual-specific phosphatase causes cell-cycle arrest and senescence. *Nat Cell Biol*. 2006;8(5):524–531.

26. Jeffrey KL, Camps M, Rommel C, Mackay CR. Targeting dual-specificity phosphatases: manipulating MAP kinase signalling and immune responses. *Nat Rev Drug Discov*. 2007;6(5):391–403.

27. Su B, Bu Y, Engelberg D, Gelman IH. SSeCKS/Gravin/AKAP12 inhibits cancer cell invasiveness and chemotaxis by suppressing a protein kinase C-Raf/MEK/ERK pathway. *J Biol Chem*. 2010; 285(7):4578–4586.

28. Shintani Y, Hollingsworth MA, Wheelock MJ, Johnson KR. Collagen I promotes metastasis in pancreatic cancer by activating c-Jun NH(2)-terminal kinase 1 and up-regulating N-cadherin expression. *Cancer Res*. 2006;66(24):11745–11753.

29. Srinivasan R, et al. Erk1 and Erk2 regulate endothelial cell proliferation and migration during mouse embryonic angiogenesis. *PLoS One*. 2009; 4(12):e8283.

30. Maraver A, et al. Therapeutic effect of gamma-secretase inhibition in Kras(G12V)-driven non-small cell lung carcinoma by derepression of DUSP1 and Inhibition of ERK. *Cancer Cell*. 2012; 22(2):222–234.

31. Henkens R, et al. Cervix carcinoma is associated with an up-regulation and nuclear localization of the dual-specificity protein phosphatase VHR. *BMC Cancer*. 2008;8:147.

32. Shedden K, et al. Gene expression-based survival prediction in lung adenocarcinoma: a multi-site, blinded validation study. *Nat Med*. 2008;14(8):822–827.

33. Wang T, et al. The histone demethylases Jhdm1a/1b enhance somatic cell reprogramming in a vitamin-C-dependent manner. *Cell Stem Cell*. 2011; 9(6):575–587.

34. Weinstein IB, Joe A. Oncogene addiction. *Cancer Res*. 2008;68(9):3077–3080

35. Dhar SS, et al. Trans-tail regulation of MLL4-catalyzed H3K4 methylation by H4R3 symmetric dimethylation is mediated by a tandem PHD of MLL4. *Genes Dev*. 2012;26(24):2749–2762.

36. Alam H, Kundu ST, Dalal SN, Vaidya MM. Loss of keratins 8 and 18 leads to alterations in alpha-6beta4-integrin-mediated signalling and decreased neoplastic progression in an oral-tumour-derived cell line. *J Cell Sci*. 2011;124(pt 12):2096–2106.